

The effects of heat release on the energy exchange in reacting turbulent shear flow

By D. LIVESCU, F. A. JABER† AND C. K. MADNIA

Department of Mechanical and Aerospace Engineering, State University of New York at Buffalo,
Buffalo, NY 14260, USA

(Received 18 July 2000 and in revised form 21 June 2001)

The energy exchange between the kinetic and internal energies in non-premixed reacting compressible homogeneous turbulent shear flow is studied via data generated by direct numerical simulations (DNS). The chemical reaction is modelled by a one-step exothermic irreversible reaction with Arrhenius-type reaction rate. The results show that the heat release has a damping effect on the turbulent kinetic energy for the cases with variable transport properties. The growth rate of the turbulent kinetic energy is primarily influenced by the reaction through temperature-induced changes in the solenoidal dissipation and modifications in the explicit dilatational terms (pressure–dilatation and dilatational dissipation). The production term in the scaled kinetic energy equation, which is proportional to the Reynolds shear stress anisotropy, is less affected by the heat release. However, the dilatational part of the production term increases during the time when the reaction is important. Additionally, the pressure–dilatation correlation, unlike the non-reacting case, transfers energy in the reacting cases, on the average, from the internal to the kinetic energy. Consequently, the dilatational part of the kinetic energy is enhanced by the reaction. On the contrary, the solenoidal part of the kinetic energy decreases in the reacting cases mainly due to an enhanced viscous dissipation. Similarly to the non-reacting case, it is found that the direct coupling between the solenoidal and dilatational parts of the kinetic energy is small. The structure of the flow with regard to the normal Reynolds stresses is affected by the heat of reaction. Compared to the non-reacting case, the kinetic energy in the direction of the mean velocity decreases during the time when the reaction is important, while it increases in the direction of the shear. This increase is due to the amplification of the dilatational kinetic energy in the x_2 -direction by the reaction. Moreover, the dilatational effects occur primarily in the direction of the shear. These effects are amplified if the heat release is increased or the reaction occurs at later times. The non-reacting models tested for the explicit dilatational terms are not supported by the DNS data for the reacting cases, although it appears that some of the assumptions employed in these models hold also in the presence of heat of reaction.

1. Introduction

Turbulent combustion is a complex physico-chemical phenomenon which is spatially three-dimensional and is of transient nature. This phenomenon has been the

† Present address: Department of Mechanical Engineering, Michigan State University, East Lansing, Michigan 48824-1226, USA.

subject of intense research over the past sixty years and continues to be of high priority in view of the worldwide concern about energy and pollution control (Givi 1989; Pope 1990; Libby & Williams 1994; Vervisch & Poinso 1998). Turbulent flows with 'non-premixed' reactants are in use in the majority of practical combustion systems. Examples are, to name a few, gas and oil furnaces and burners, diesel engines, and hypersonic propulsion systems.

The intricate interactions between turbulence and chemical reaction occur over a broad spectrum of length and time scales and involve many different quantities. Our lack of adequate understanding of these interactions places severe limitations on the modelling of chemically reactive turbulent flows. For example, most of the existent turbulence closures which are used for reacting flow calculations are based on those developed for non-reacting flows. These closures are potentially limited and do not account for important characteristics of the turbulent combustion such as the extensive density and molecular property variations, significant dilatational turbulent motions, etc.

Theoretical studies of compressible turbulence were performed as early as 50 years ago; however much less is known in comparison with incompressible turbulence. Kovaszny (1953) studied the linearized equations of compressible turbulence and identified the existence of three basic modes: the vorticity, acoustic and entropy modes. Chu & Kovaszny (1958) extended the analysis to first-order interaction terms and examined the weakly nonlinear interaction between the modes. However, it is not clear how this analysis can be extended to fully nonlinear turbulence (Blaisdell, Mansour & Reynolds 1993).

Moyal (1951) introduced the decomposition of the velocity field in Fourier space into a solenoidal and a dilatational part and showed that the two fields interact only through nonlinear terms for isotropic turbulence. Such a decomposition has been exploited by rapid distortion theories in studies of shock-turbulence interaction and homogeneous turbulence subjected to bulk compression or uniform mean shear (for a review see Lele 1994).

Direct numerical simulation (DNS) is becoming a powerful investigative tool to study compressible turbulence. This method has enabled the examination of turbulent flows in a temporally and spatially accurate manner without the need for turbulence modelling (Givi & Madnia 1992; Givi 1994; Moin & Mahesh 1998). Moreover, recently it has been successfully employed in simulating laboratory experiments on turbulent mixing (Livescu, Jaber & Madnia 2000). An assumption usually made in DNS of turbulent flows is that the flow is homogeneous. This idealization is unable to retain some important aspects of inhomogeneous compressible flows such as mean density variations or acoustic radiation to the far field. However, it allows the study of some effects of compressibility that are shared by different types of turbulent flows.

DNS of non-reacting isotropic compressible turbulence has been performed by several investigators. Kida & Orszag (1990, 1992) considered the transport equations of the solenoidal and dilatational parts of the turbulent kinetic energy and showed that their direct coupling is weak. Erlebacher *et al.* (1990) decomposed the pressure fluctuations into a compressible and an incompressible part and discussed the equilibrium between the kinetic and potential energies of the compressible component for two-dimensional turbulence. This analysis is extended to the three-dimensional case by Sarkar *et al.* (1991b).

There have been several previous numerical studies of homogeneous non-premixed reacting flows (Givi 1989; Vervisch & Poinso 1998). The heat release effects on compressible isotropic forced and decaying turbulence are considered by Mahalingam,

Chen & Vervisch (1995), Balakrishnan, Sarkar & Williams (1995), Jaber & Madnia (1998), Martin & Candler (1998) and Jaber, Livescu & Madnia (2000). It is shown that the heat release influences the dilatational and solenoidal fluid motions differently. Thus, the localized expansions which occur due to an exothermic reaction increase the dilatational turbulent kinetic energy. Moreover, if the reaction rate is temperature dependent then there is a feedback mechanism between the chemical reaction and the turbulent motions.

The next level of complexity over the isotropic turbulence is the homogeneous shear flow. Since mean shear is present in most turbulent flows, the study of homogeneous shear flow can reveal some important features of compressibility in practical turbulent flows. Experimental results concerning homogeneous shear flow are available only for the incompressible case (Tavoularis & Corrsin 1981; Tavoularis & Karnik 1989; Souza, Nguyen & Tavoularis 1995; Garg & Warhaft 1997).

Nomura & Elghobashi (1992) and Leonard & Hill (1992) studied the mixing and chemical reaction in isotropic and homogeneous sheared incompressible flows. The non-reacting compressible homogeneous shear flows have been studied numerically by Feieresen *et al.* (1982), Sarkar, Erlebacher & Hussaini (1991a), Blaisdell *et al.* (1993), Sarkar (1995), Blaisdell, Coleman & Mansour (1996), Simone, Coleman & Cambon (1997), Hamba (1999). It was found that the turbulent kinetic energy increases almost exponentially after an initial development time and that the compressibility has a stabilizing effect on the growth of the turbulent motion. The reduced growth rate for higher values of the turbulent Mach number, M_T , or shear rate, S , is the result of less efficient turbulent production and an increase in the dissipation rate. Additionally, the ratio of the dilatational to solenoidal dissipation, χ_ϵ , becomes independent of the initial conditions and exhibits a M_T^2 dependence. The normalized pressure and density fluctuations are also proportional to M_T^2 (Sarkar *et al.* 1991a). The effect of compressibility on the growth of the turbulent kinetic energy is similar to the behaviour observed in experiments and simulations of compressible mixing layers and wakes (Dimotakis 1991; Sandham & Reynolds 1989; Chen, Cantwell & Mansour 1989; Sarkar 1995).

The results of the previous studies, as briefly mentioned above, reveal many interesting features of turbulent compressible non-reacting and isotropic chemically reacting flows. However, the complex role played by the combined influence of the turbulence and the chemical reaction in compressible fluid medium is not fully understood. Moreover, there are no available DNS data for the case of compressible reacting homogeneous shear flow.

The present study thus aims to identify: (i) the changes in the structure of the reacting compressible homogeneous turbulent shear flow due to the heat release, (ii) the energy transfer among different components of the turbulent kinetic energy and internal energy responsible for these changes, and (iii) the performance of the existing non-reacting models for the explicit dilatational terms in the turbulent kinetic energy equation for the reacting case.

This paper is organized as follows. Section 2 contains the governing equations and the numerical methodology. The heat release effects on the energy exchange among different types of energy are presented in §3. In §3.1 the transport equations for the turbulent kinetic, internal and total energies are discussed. Also in this section some non-reacting models for the pressure–dilatational correlation are assessed. Since the heat release strongly influences the explicit dilatational terms in the kinetic energy equation, in §3.2 the transport equations for the dilatational and solenoidal components of the kinetic energy are examined. The DNS data are also used to

evaluate models for the dilatational dissipation. Due to the anisotropy of the flow, the kinetic energy in each direction is affected differently by the reaction. Consequently, the transport equations for the kinetic energy components in each coordinate direction are studied in § 3.3. Also in this section the behaviour of the production of the turbulent kinetic energy is analysed by considering the transport equation for the Reynolds shear stress anisotropy. In order to explain some of the findings, in § 3.4 the transport equations for the solenoidal and dilatational parts of the kinetic energy in each coordinate direction are examined. A summary and conclusions are given in § 4.

2. Problem formulation and computational methodology

2.1. Governing equations

The conservation equations governing a compressible flow in a continuum medium undergoing chemical reaction are the continuity, momentum transport, energy and species-mass-fraction transport equations (Williams 1995; Livescu 2001). These equations are non-dimensionalized by the initial r.m.s. velocity fluctuations (u_0), initial mean temperature (T_0), initial mean density (ρ_0) and a reference length scale (l_0) related to the computational box size. The instantaneous velocity is decomposed into a mean (\tilde{u}_i) and a fluctuating (u_i'') part using the Favre average (Favre 1965). Although in homogeneous flows the Favre averaging and Reynolds or ensemble averaging of the velocity field are equivalent, the formal distinction between the two averages is maintained throughout the paper. The volumetric-averaged density $\langle \rho \rangle$, pressure $\langle p \rangle$, and temperature $\langle T \rangle$ are uniform in space, conditions necessary and sufficient to preserve the homogeneity for a non-reacting flow (Feieresen *et al.* 1982; Blaisdell, Mansour & Reynolds 1991). For reacting flows, the nonlinear nature of the source terms in the scalar and energy transport equations gives rise to a supplementary condition for maintaining the homogeneity. This condition is fulfilled only when the mean mass fractions are uniform in space, for all species considered.

After applying Rogallo's transformation of coordinates (Rogallo 1981), $x'_i = B_{ij}(t)x_j$, where the transformation matrix has constant diagonal components β_i and the only non-zero off-diagonal component is $B_{12} = -\beta_1 St$, the conservation equations for a calorically perfect fluid satisfying Stokes' hypothesis become (Livescu 2001)

$$\frac{\partial \rho}{\partial t} + \frac{\partial}{\partial x'_k} (\rho u''_j) B_{kj} = 0, \quad (2.1)$$

$$\begin{aligned} \frac{\partial}{\partial t} (\rho u''_i) = & -\rho u''_2 S \delta_{i1} - \frac{\partial}{\partial x'_k} (\rho u''_i u''_j) B_{kj} - \frac{\partial}{\partial x'_k} p B_{ki} \\ & + \frac{\partial}{\partial x'_k} \left(\tau_{ij} + \frac{\mu}{Re_0} (S \delta_{i1} \delta_{j2} + S \delta_{i2} \delta_{j1}) \right) B_{kj}, \end{aligned} \quad (2.2)$$

$$\begin{aligned} \frac{\partial}{\partial t} (\rho \phi) = & S(\tau_{12} - \rho u''_1 u''_2) - \frac{\partial}{\partial x'_k} (\rho u''_j \phi) B_{kj} - \frac{\partial}{\partial x'_k} (p u''_j) B_{kj} \\ & + \frac{\partial}{\partial x'_k} (\tau_{ij} u_i) B_{kj} + \frac{1}{(\gamma - 1) M_0^2 Re_0 Pr} \frac{\partial}{\partial x'_k} \left(\mu \frac{\partial T}{\partial x'_l} B_{lj} \right) B_{kj} + Q, \end{aligned} \quad (2.3)$$

$$\frac{\partial}{\partial t} (\rho Y_\alpha) = -\frac{\partial}{\partial x'_k} (\rho u''_j Y_\alpha) B_{kj} + \frac{1}{Re_0 Sc} \frac{\partial}{\partial x'_k} \left(\mu \frac{\partial Y_\alpha}{\partial x'_l} B_{lj} \right) B_{kj} + w_\alpha, \quad (2.4)$$

where $S = \partial \tilde{u}_1 / \partial x_2$, $\tau_{ij} = (2\mu / Re_0)(s_{ij} - \frac{1}{3}\Delta\delta_{ij})$, $s_{ij} = \frac{1}{2}((\partial u_i'' / \partial x_k') B_{kj} + (\partial u_j'' / \partial x_k') B_{ki})$ is the strain rate tensor and $\Delta = (\partial u_i'' / \partial x_k') B_{ki}$ is the dilatation of the velocity fluctuations. The primary transport variables are the density ρ , velocity fluctuations in the x_i -direction u_i'' , modified total energy $\phi \equiv p / (\rho(\gamma - 1)) + \frac{1}{2}u_i''u_i''$, where $\gamma = 1.4$ is the ratio of the specific heats and p is the instantaneous pressure ($p = \langle p \rangle + p'$ with p' the pressure fluctuations), and Y_α is the species mass fractions. The pressure is non-dimensionalized by $\rho_0 u_0^2$ such that the non-dimensional form of the ideal gas equation of state becomes $p = \rho T / \gamma M_0^2$.

The non-dimensional parameters in equations (2.1)–(2.4) are the computational Reynolds number, $Re_0 = \rho_0 u_0 l_0 / \mu_0$, the Prandtl number, $Pr = \mu_0 c_p / \kappa_0$, the Schmidt number, $Sc = \mu_0 / \rho_0 D_0$, and the reference Mach number, $M_0 = u_0 / \sqrt{\gamma R T_0}$, where R is the gas constant. The reference viscosity, μ_0 , thermal diffusivity, κ_0 , and mass diffusivity, D_0 , are assumed to be proportional to T_0^n and in all cases the Lewis number is unity with $Pr = Sc = 0.7$. Also, in all simulations $Re_0 = 180$. The non-dimensional viscosity, μ , is modelled by assuming a power-law temperature dependence, $\mu = T^n$.

The chemical, w_α , and heat, Q , source terms are modelled by assuming a single-step irreversible reaction $A + rB \rightarrow (1 + r)P$ ($r = 1$ in this study) with Arrhenius-type reaction rate

$$\left. \begin{aligned} w_A &= \frac{1}{r} w_B = -\frac{1}{1+r} w_P = -Da \rho^2 Y_A Y_B \exp(-Ze/T), \\ Q &= \frac{Ce}{(\gamma - 1)M_0^2} w_P. \end{aligned} \right\} \quad (2.5)$$

The field is composed of the reactants A , B and product P , so the index α in equation (2.4) corresponds to A , B or P and $Y_P = 1 - Y_A - Y_B$. The non-dimensional quantities affecting the chemistry are the heat release parameter, $Ce = -H^0 / c_p T_0$, the computational Damköhler number, $Da = K_f \rho_0 l_0 / M_m u_0$, and the Zeldovich number, $Ze = E_a / R_u T_0$, and are assumed to be constant. Here, $-H^0$ is the heat of reaction, K_f is the reaction rate parameter, M_m is the molar mass, R_u is the universal gas constant, and E_a is the activation energy.

2.2. Numerical solution procedure

Equations (2.1)–(2.4) are integrated using the Fourier pseudo-spectral method (Gottlieb & Orszag 1977; Givi 1994) with triply periodic boundary conditions. The variables are time advanced in physical space using a second-order-accurate Adams–Bashforth scheme. All simulations are performed within a box containing 128^3 grid points. The computational domain is twice as long in the streamwise direction as in the cross-stream and spanwise directions in order to account for the elongated turbulent structures due to the presence of the shear (Rogers, Moin & Reynolds 1987; Blaisdell *et al.* 1991). Because the computational domain should become $2\pi \times 2\pi \times 2\pi$ after the transformation of coordinates, this yields $\beta_1 = 0.5$, $\beta_2 = 1.0$ and $\beta_3 = 1.0$. The transformation of coordinates also makes necessary a periodic remeshing of the grid in order to avoid errors associated with highly skewed grids. For the computational domain used this is done at $St = 2m - 1$ (where m is a positive integer) such that no interpolation onto the new domain is needed. In order to avoid aliasing errors, the remeshing procedure is carried out in wavenumber space. Aliasing errors are also generated at the evaluation of nonlinear terms. These errors are controlled by writing the convective terms from equations (2.2)–(2.4) in the skew-symmetric form which minimizes the aliasing errors (Blaisdell *et al.* 1993). Also, the range of parameters

which control the flow field are chosen in such a way that the magnitudes of the unresolved Fourier modes formed at the evaluation of the nonlinear terms are small.

2.3. Initial conditions and test case

The velocity fluctuations field is initialized as a random, solenoidal, three-dimensional field with Gaussian spectral density function and unity r.m.s. The location of the peak of this spectrum is $k_0 = 10$ for all simulations. The density and temperature fields are non-dimensionalized by their initial mean value, so the mean non-dimensional initial density and temperature are set to one. The initial density field has no fluctuations and, therefore, the average initial pressure can be computed from the mean equation of state, $\langle p \rangle = \langle \rho \rangle \langle T \rangle / \gamma M_0^2$. The initial pressure fluctuations are evaluated from a Poisson equation.

In order to test the influence of the initial conditions on the results presented in this paper, the reacting and non-reacting base runs (see below) were also performed by extending the initialization of the velocity and thermodynamic fields proposed for isotropic turbulence by Ristorcelli & Blaisdell (1997) to the case of homogeneous shear flow. As before, the initial pressure fluctuations are evaluated from the initial solenoidal velocity field by solving a Poisson equation. In addition, the linearization of the continuity equation provides an equation for the dilatation which yields the initial dilatational velocity field. Furthermore, the initial density and temperature fluctuations are calculated from the linear adiabatic equation of state. The results obtained using this initialization are in good agreement with our results. In general, the differences between the two initializations in all the quantities presented in this paper are less than 5% above $St = 2$.

The scalar field is initialized following the method first proposed by Eswaran & Pope (1988). Scalar A is initialized by generating a random field with Gaussian energy spectrum. The location of the peak of this spectrum is k_{0s} which is used to control the initial length scale of the scalar field. The scalar field generated is transformed into physical space where all negative values are set to -1 and all positive values to 1 . The result is a field with double-delta PDF which is smoothed by applying a filter function to decrease the weights at high wavenumbers. The physical values of the scalar are no longer bounded by ± 1 and, in order to reduce their amplitude, the field is allowed to go through molecular diffusion. Finally, the interval $[-1, 1]$ is mapped onto $[0, 1]$ to obtain the scalar mass fractions. The resulting scalar field has a mean of 0.5 and a length scale controlled by the peak of the initial Gaussian energy spectrum. Scalar B is perfectly anti-correlated with A and there is no P in the domain at initial time.

The computer code developed for this work was validated by running a non-reacting simulation, case scb96 from Blaisdell *et al.* (1991). For the reacting case, the code was tested against isotropic simulations performed in earlier studies by the authors (Jaber & Madnia 1998; Jaber *et al.* 2000).

3. Energy exchange

Direct numerical simulations of chemically reacting compressible turbulent shear flows were performed. Table 1 provides a list of the relevant information about each of the cases studied. S_0^* , Re_{λ_0} and Re_{T_0} are the initial values of the non-dimensional shear rate, $S^* = S(2K)/\epsilon$, Reynolds number based on Taylor microscale, and turbulent Reynolds number, $Re_T = ((2K)^2/\epsilon\tilde{u})Re_0$, respectively. Here $K = \frac{1}{2}\langle \rho u_i' u_i' \rangle$ is the turbulent kinetic energy and $\epsilon = \langle \tau_{ik}(\partial u_i'/\partial x_k') B_{kj} \rangle$ is the rate of dissipation of

Case	Ce	Da	k_{0s}	n
1	0	0	4	0.7
2	1.44	1100	4	0.7
3	1.44	1100	4	0.0
4	2.16	1100	4	0.7
5	1.44	500	4	0.7
6	1.44	1100	10	0.7
7	1.44	1750	4	0.7
8	0.576	1100	4	0.7

TABLE 1. Parameters for the DNS cases. $M_0 = 0.3$, $S_0^* = 7.24$, $Re_{\lambda_0} = 21$, $Re_{\tau_0} = 256$. All reacting cases have $Ze = 8$.

turbulent kinetic energy per unit volume. Cases 1 and 2 are the reference non-reacting and reacting cases, respectively. In order to isolate the influence of temperature dependence of the transport properties, a simulation with $n = 0$ (case 3) and the same parameters as the reference reacting case was performed. A non-reacting simulation with $n = 0$ was also performed. However, since the mean temperature increase for this case is very small, the results obtained are very close to those obtained for case 1. Consequently, only cases 1, 2 and 3 are used for examining the variation of the molecular transport properties with temperature. The influence of the reaction parameters Ce , Da and initial scalar length scale is considered in cases 4–8.

The reaction parameters chosen for the cases considered mimic the combustion of a typical hydrocarbon in air at low to moderate values of Reynolds number. Estimating an initial temperature $T_0 = 300$ – 1000 K which is in the range of temperatures in an internal combustion engine before the ignition, and using characteristic hydrocarbon values for μ_0 and c_p , yields $K_f \sim O(10^{14} \text{ cm}^3 \text{ mol}^{-1})$, $E_a \sim O(45 \text{ kJ mol}^{-1})$ and $-H^0 \sim O(60 \text{ kJ mol}^{-1})$, values in the range of the elementary reactions for hydrocarbon combustion (Turns 2000).

Since the purpose of this paper is to study the influence of the heat release on the energy exchange in homogeneous shear flows, only the parameters which directly influence the reaction are discussed here. However, the influence of initial Mach number ($0.1 < M_0 < 0.6$) and mean shear rate ($4.8 < S^* < 22$) was also examined and the results presented in the subsequent sections are found to be qualitatively unchanged for the range of M_0 and S^* considered.

The time evolution of the mean reaction rate ($\langle w \rangle = \langle w_P \rangle$) shown in figure 1(a) exhibits the expected behaviour for an Arrhenius reaction rate. By modifying the values of Ce , Da or k_{0s} both the magnitude and the time location of the peak of the mean reaction rate change. In turbulent reacting flows the structure of the flame is dependent on the underlying turbulent field as well as the chemistry parameters. Additionally, the reaction rate depends on the variations of the thermodynamics variables. The heat of reaction in turn affects the turbulent motions and the thermodynamic variables, hence a two-way coupling between turbulence and chemical reaction exists. In order to make meaningful comparisons among different cases, the reaction parameters are chosen such that the peak of the mean reaction rate occurs approximately at the same time for cases 4, 6 and 7 and cases 5 and 8, respectively. In addition, to further facilitate the comparisons, each case considered has the value of only one parameter different from that used for the reacting base case. Thus, for example by comparing cases 4 and 6 which have different values for the heat release parameter, Ce , but

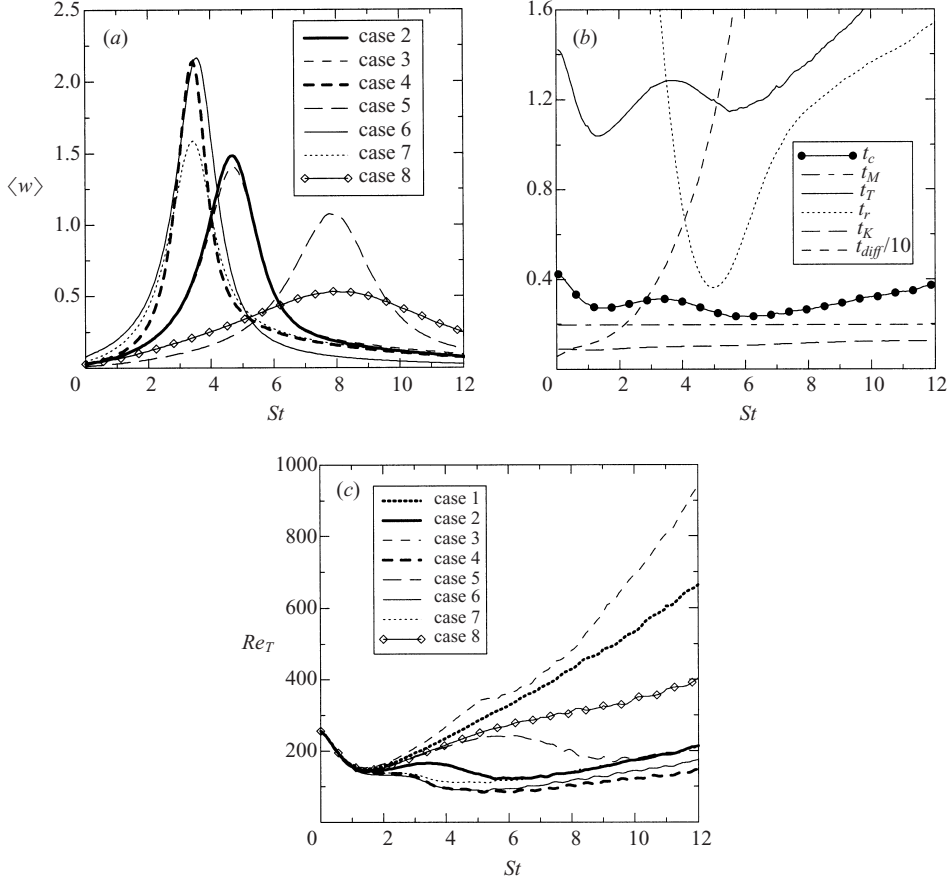


FIGURE 1. Time evolution of (a) mean reaction rate for product, (b) characteristic time scales for case 2, and (c) turbulent Reynolds number.

similar behaviour for the mean reaction rate, information about the influence of Ce can be extracted. It should be noted that, since approximately 90% of the reactants are consumed before the end of the simulation, Ce is directly proportional to the total amount of heat injected in the flow. Furthermore, a comparison between cases 6 and 7 with the same Ce isolates the effects of the magnitude of the mean reaction rate peak.

The reaction parameters are chosen such that the peak of the mean reaction rate occurs after the kinetic energy starts to grow (see figure 2). Furthermore, the heat release was kept above a certain value so that the mean reaction rate exhibits a well-defined peak. The simulations presented are stopped at $St = 12$, following the consumption of almost all the reactants. Additionally, the compressible scales remain small compared to the box size at all times (Livescu 2001).

In order to evaluate how fast the reaction is, figure 1(b) compares the characteristic reaction time ($t_r \equiv \langle \rho Y_P \rangle / \langle w_P \rangle$), the acoustic time ($t_c \equiv (2K)^{3/2} / (\epsilon \langle c \rangle)$), the Kolmogorov time ($t_K \equiv \sqrt{\langle \mu \rangle} / (Re_0 \langle \rho \rangle \epsilon)$), the turbulent time ($t_T \equiv 2K / \epsilon$), the time scale of the mean velocity ($t_M \equiv 1/S$) and the diffusion time ($t_{diff} \equiv 1/\tilde{\chi}_{st}$) for case 2. Here $\langle c \rangle$ is the mean speed of sound and $\tilde{\chi}_{st} = \langle 2\mu / (Re_0 Sc) \nabla Z \cdot \nabla Z |_{Z=Z_{st}} \rangle$ is the mixture fraction dissipation taken at the stoichiometric surface. As expected, the diffusion

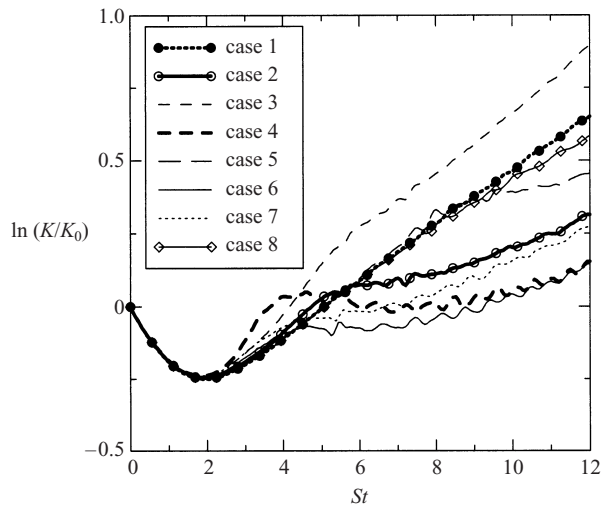


FIGURE 2. Temporal variation of the turbulent kinetic energy.

time scale is much larger than the other characteristic times. The reaction time scale is greater than the Kolmogorov time scale at all times, although they become close at the time when the mean reaction rate peaks. The characteristic time of the mean flow is always close to the acoustic time. Similar results are obtained for the other runs considered. For cases 4 and 6, the minimum values of t_r decrease, but remain larger than the acoustic time scale.

Since the chemical reaction significantly increases the temperature and consequently the values of the molecular viscosity, it is useful to examine the time evolution of Re_T . Figure 1(c) shows that in the absence of heat release, Re_T grows continuously after a development time. All the reacting cases with variable transport properties have lower values of Re_T than the non-reacting case. A comparison between cases 2 and 3 indicates that the values of Re_T decrease when the reaction becomes important due to the variation of the transport properties with temperature.

The rest of this section is organized as follows: first the energy exchange between the kinetic and internal energies is discussed; then the kinetic energy is decomposed into different components and the energy exchange among them is examined.

3.1. Kinetic, internal and total energies

The evolution of the turbulent kinetic energy in non-reacting homogeneous compressible shear flow has been studied by several authors (Blaisdell *et al.* 1993; Sarkar 1995; Simone *et al.* 1997; Hamba 1999). The results obtained for case 1 (figure 2) are in agreement with the previous results and exhibit typical behaviour for a non-reacting flow. Since the initial velocity field is isotropic, the production term in the turbulent kinetic energy equation ($\langle -\rho u_1'' u_2'' S \rangle$) is zero at the beginning of the simulation and the turbulence decays. As the flow develops, the anisotropy of the flow increases and the production eventually outweighs the dissipation rate, such that the turbulent kinetic energy grows. The experimental (Tavoularis & Karnik 1989) and numerical (Rogers *et al.* 1987) results obtained for incompressible shear flow suggest an exponential growth rate for K . Although a quasi-exponential growth rate was also obtained at later times in compressible shear flow (Blaisdell *et al.* 1993) it is well known that the growth of the turbulent kinetic energy is not universal and is affected by the

compressibility (Sarkar 1995; Simone *et al.* 1997; Hamba 1999). However, for the time range simulated, case 1 exhibits a nearly exponential growth of the turbulent kinetic energy (figure 2).

In the presence of heat release, the growth of the turbulent kinetic energy is significantly modified. For all reacting cases with variable transport properties K decreases compared to the non-reacting case, after the time when the mean reaction rate peaks. However, there is a short period of time when K has a larger magnitude than for case 1. This effect, significant in case 4, is shown in the next section to be related to the different behaviour of the solenoidal and dilatational kinetic energies under the influence of heat release. Furthermore, the time evolution of K is very different for case 3 with constant transport properties compared to case 2. Thus, as the mean reaction rate becomes significant, the growth rate of K for case 3 increases compared with the non-reacting case. Consequently, the values of K are higher for case 3 than for case 1.

In order to examine the energy transfer leading to the modifications in the rate of growth of the turbulent kinetic energy in the presence of the heat of reaction, the transport equations for turbulent kinetic (K), internal ($E_t \equiv \langle \rho e_t \rangle = \langle p \rangle / (\gamma - 1)$), and modified total ($E_t \equiv \langle \rho \phi \rangle$) energies are considered. All the terms in the equations are scaled by SK in order to make a meaningful comparison between the reacting and non-reacting cases:

$$\frac{1}{K} \frac{d}{d(St)} K = P + PD + VD + VD1, \quad (3.1)$$

$$\frac{1}{K} \frac{d}{d(St)} E_t = -PD - VD + HR - VD1 + VD2, \quad (3.2)$$

$$\frac{1}{K} \frac{d}{d(St)} E_t = P + HR + VD2, \quad (3.3)$$

where PD , P , VD and HR represent the pressure–dilatation, production, viscous dissipation and the heat release, respectively. The terms $VD1$ and $VD2$ are viscous-dissipation terms which arise due to the interaction with the mean flow. The definitions of the terms in equations (3.1)–(3.3) are presented in Appendix A. The pressure–dilatation and viscous-dissipation terms transfer energy between K and internal energy and their net effect on E_t is zero. The heat release term is much larger than the other terms in equation (3.2) for the reacting cases considered in this study and thus the magnitude of the internal energy is much larger than that of the kinetic energy. The simulations show, for all cases considered, that the terms involving fluctuations of the viscosity are negligible. It should be noted that the mean kinetic energy does not vary with time and hence equation (3.3) also represents the transport equation for the total energy.

The growth rate of the turbulent kinetic energy, as discussed above, is not directly dependent on the heat release. However, the terms in equation (3.1) are affected by the change in the internal energy. Figure 3(a) compares the time evolution of the terms in equation (3.1) for cases 1–3. For non-reacting shear flow, Sarkar (1995) showed that the production term is affected by compressibility and is responsible for the decrease in the growth of turbulent kinetic energy at higher Mach numbers or shear rate values. However, a comparison among the base cases indicates that the heat of reaction does not have a significant influence on the evolution of the production term. The same behaviour is obtained for the other cases considered and it is explained by examining the terms in the transport equation for the Reynolds

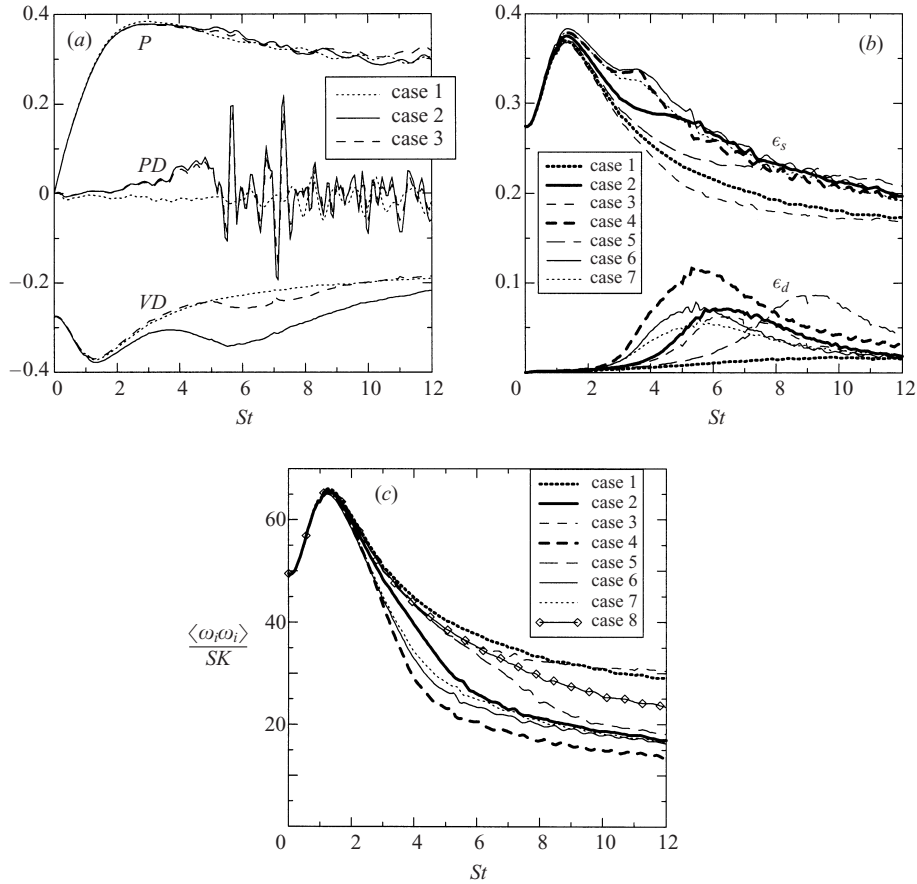


FIGURE 3. Evolution of (a) terms in the scaled kinetic energy equation (3.1), (b) dilatational and solenoidal dissipations, and (c) normalized enstrophy.

shear stress anisotropy (§ 3.3). At higher values of shear rate S^* , the production term increases slightly during the time when the reaction is important, but it remains less affected than the other terms in the kinetic energy equation.

The magnitude of the viscous-dissipation term increases significantly for case 2 compared to the non-reacting case and increases slightly if the transport properties do not vary with temperature. The influence of heat release on the viscous-dissipation term can be further examined by considering the usual decomposition into a term proportional to the mean enstrophy, ϵ_s (solenoidal dissipation), and a term proportional to the mean-squared dilatation, ϵ_d (dilatational dissipation), as shown in Appendix A. The time evolution of these terms, presented in figure 3(b), shows that the dissipation occurs primarily through the vortical motion in both the reacting and non-reacting cases. The dilatational dissipation is significantly enhanced by the heat of reaction. This effect is amplified if the heat release parameter is increased (compare case 4 with cases 6 and 7) or the reaction takes place at later times (compare cases 2, 5 and 7). The temperature dependence of the transport properties does not appear to have an important influence on the dilatational dissipation since the results obtained for cases 2 and 3 are close.

On the other hand, the results presented in figure 3(b) indicate that the solenoidal

dissipation is affected by the heat release primarily through the variation of the transport properties with temperature (compare case 1, 2 and 3). Moreover, the magnitude of ϵ_s is increased by the reaction for all cases with variable transport properties. However, the value of Ce does not appear to influence significantly this increase since the results obtained for case 4 and cases 6 and 7 are close. The heat of reaction influences the viscous-dissipation term through the changes in the viscosity and the small-scale turbulent motions. Thus, the solenoidal dissipation depends on the average viscosity and the mean enstrophy. The average viscosity, $\langle\mu\rangle$, depends only on the mean temperature, which increases due to reaction, and its final value is proportional to the amount of heat injected in the flow. Consistent with the decaying turbulence results of Jaber *et al.* (2000), the energy spectra of the solenoidal velocity component indicate that the small solenoidal scales decrease their energy for the reacting cases with variable transport properties. As a result, the mean enstrophy, which is a measure of the small scales of the solenoidal velocity, decreases for the reacting cases compared to the non-reacting case (figure 3c). Additionally, figure 3(c) indicates that as Ce increases (and consequently the mean temperature) the mean enstrophy decreases. Consistent with the results of Jaber *et al.* (2000), the values of the scaled mean enstrophy are not significantly different for cases 1 and 3, suggesting that the heat release influences the mean enstrophy mainly due to the variations in the molecular transport coefficients. Since $\langle\mu\rangle$ and the scaled mean enstrophy are oppositely affected by the value of Ce , ϵ_s depends weakly on the heat release parameter.

The pressure–dilatation term oscillates around zero and exchanges energy between E_I and K (figure 3a). In the non-reacting case, the amplitude of the oscillations of PD is small at early times and increases as the kinetic energy grows. In cases 2 and 3, as the mean reaction rate increases the pressure–dilatation does not oscillate much and its magnitude is positive. However, after the mean reaction rate peaks, the oscillations of PD are greatly enhanced. These oscillations increase their amplitude if Ce is increased. A comparison between the results for cases 2 and 3 indicates that the variation in transport properties has little effect on the evolution of the pressure-dilatation term, similar to the results obtained for isotropic turbulence by Jaber *et al.* (2000).

Since the values of PD oscillate around zero, its time-integrated values can provide information about its average behaviour and help in understanding its contribution to the variation of K . Figure 4 shows that, on average, the scaled pressure–dilatation correlation has a different role in the reacting and non-reacting cases. In agreement with the previous simulations of compressible non-reacting shear flows (Blaisdell *et al.* 1993; Sarkar *et al.* 1991a; Sarkar 1995) PD transfers energy, on average, from the kinetic energy to the internal energy. On the contrary, in the presence of heat release, the results indicate that the average contribution of PD to the change of the kinetic energy increases as Ce increases and becomes positive if the heat release is significant. After the magnitude of the mean reaction rate becomes small (figure 1a), the time-averaged values of PD do not decrease and the long-time results obtained for cases 2, 5, 6 and 7 (same value of Ce) are close. The behaviour of the pressure–dilatation term in the turbulent reacting shear flow found here is also similar to that found in numerical simulations of reacting isotropic turbulence (Martin & Candler 1998; Jaber *et al.* 2000).

To summarize, the heat release has a significant influence on the energy exchange between the internal and turbulent kinetic energies. Thus, the contribution from the pressure-dilatation term increases and changes the direction of energy transfer in

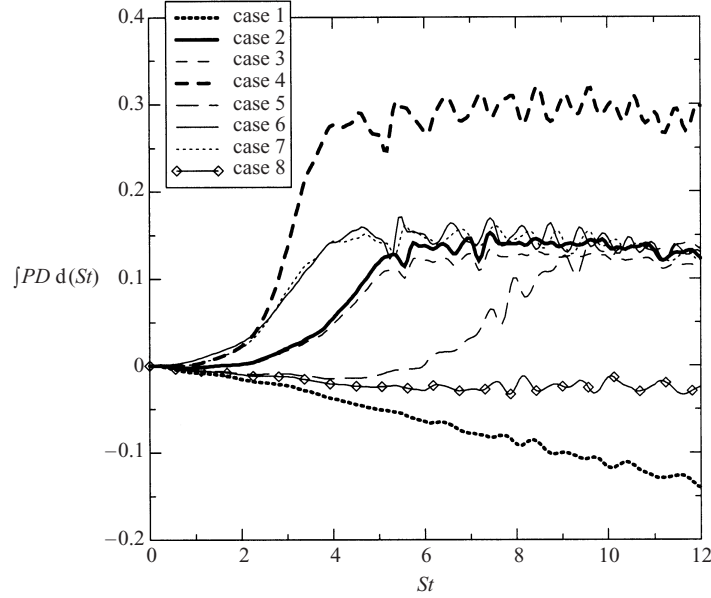


FIGURE 4. Time-integrated values of the pressure-dilatation.

the reacting cases with significant heat release. The contribution from the viscous dissipation term increases significantly in cases with variable transport properties and, since the contribution from the production term to the change of the kinetic energy is slightly affected by the heat release, it can be concluded that the enhanced dissipation is responsible for the reduced growth of the kinetic energy in these cases. On the other hand, the contribution from the viscous-dissipation term increases in case 3 compared to case 1, so that the pressure-dilatation term is responsible for the higher rate of growth of kinetic energy in case 3.

The pressure-dilatation correlation was modelled in non-reacting homogeneous flows by Durbin & Zeman (1992) using the assumption

$$\langle p' \Delta \rangle = -\frac{1}{2\gamma \langle p \rangle} \frac{d\langle p'^2 \rangle}{dt}. \quad (3.4)$$

This relation can be obtained by starting from the linearized equations (Kovaszny 1953; Blaisdell *et al.* 1993) and combining the continuity and entropy equations, as was done by Durbin & Zeman (1992). Alternatively, one can consider the exact transport equation for the pressure variance, which, for the case of homogeneous reacting shear flow, can be written as

$$\begin{aligned} \frac{d\langle p'^2 \rangle}{dt} = & \underbrace{-2\gamma \langle p \rangle \langle p' \Delta \rangle}_I - \underbrace{(2\gamma - 1) \langle p'^2 \Delta \rangle}_II \\ & + \underbrace{\frac{2}{M_0^2 Re_0 Pr} \left\langle p' \frac{\partial}{\partial x'_m} \left(\mu \frac{\partial T}{\partial x'_n} B_{ni} \right) B_{mi} \right\rangle}_III \\ & + \underbrace{\frac{4(\gamma - 1)}{Re_0} \left\langle p' \mu \left(s_{ij} s_{ij} - \frac{\Delta^2}{3} + 2s_{12} S + \frac{S^2}{2} \right) \right\rangle}_IV + \underbrace{\frac{2Ce}{M_0^2} \langle p' w_p \rangle}_V. \end{aligned} \quad (3.5)$$

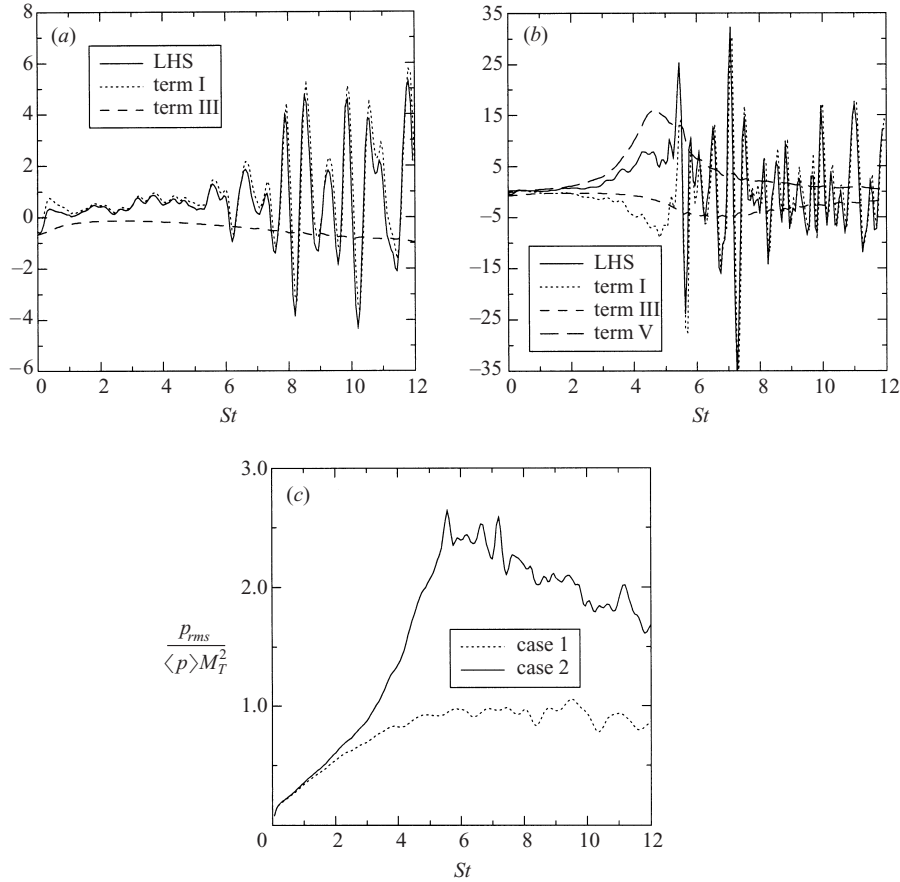


FIGURE 5. Evolution of the terms in the pressure variance equation (3.5) for (a) case 1 and (b) case 2. (c) Temporal variation of the normalized values of the r.m.s. pressure.

Consistent with the previous studies (Sarkar *et al.* 1991a; Hamba 1999), for the non-reacting case only terms I (proportional to the product between mean pressure and pressure–dilatation correlation) and III (correlation between pressure fluctuations and temperature diffusion) are important. Figure 5(a) shows, however, that term III varies much slower in time than term I for case 1. Furthermore, since the magnitude of term III is much smaller than the peak values of term I, equation (3.4) represents a good approximation for the pressure–dilatation. For the reacting case, term V becomes significant as the mean reaction rate increases (figure 5b). During this time, Durbin & Zeman’s (1992) assumption ceases to hold. Later, as the mean reaction rate decreases, term III balances term V. Consequently, equation (3.4) becomes a good approximation for $\langle p'\Delta \rangle$.

The next assumption of Durbin & Zeman (1992) is that the normalized pressure variance relaxes to an equilibrium value on the acoustic time scale. This equilibrium value is a function of the turbulent Mach number. Although t_r is much larger than t_c most of the time for the cases considered, the addition of heat prevents the pressure variance being modelled in terms of Mach number only. In particular, figure 5(c) shows that although $p_{rms}/\langle p \rangle$ scales with M_T^2 in the non-reacting case, in agreement with the results of Sarkar *et al.* (1991a), it has a very different behaviour in the

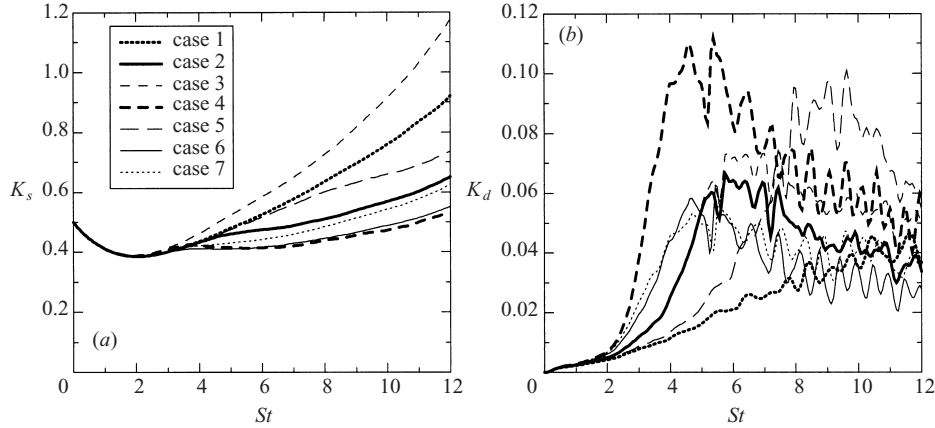


FIGURE 6. Temporal variation of (a) solenoidal turbulent kinetic energy and (b) dilatational kinetic energy.

presence of heat release. Consequently, in order to properly model the evolution of the pressure variance in the reacting case, the model should consider the amount of heat injected into the flow.

3.2. Solenoidal and dilatational components of the turbulent kinetic energy

It is shown in the previous section that the heat of reaction influences the growth of the kinetic energy primarily through explicit dilatational effects (pressure–dilatational correlation and dilatational dissipation) and temperature-induced changes in the solenoidal viscous dissipation. This suggests that the solenoidal and dilatational motions are influenced differently by the heat of reaction. In order to further examine this influence, $W_i = \sqrt{\rho}u_i''$ is decomposed into its solenoidal, dilatational, and mean parts (Kida & Orszag 1990, 1992; Jaber & Madnia 1998; Jaber *et al.* 2000). Consequently, the kinetic energy components are defined as $K_\alpha = \frac{1}{2}\langle |W_\alpha|^2 \rangle$, where $\alpha \equiv s, d, o$ denotes the solenoidal, dilatational, and mean components of W_i (and of the kinetic energy), respectively. This decomposition accounts for the density fluctuations, which can become important in the presence of heat release. For all cases considered, K_o is negligible compared to K_s and K_d .

Figure 6(a) shows that the solenoidal kinetic energy increases faster in case 3 than in case 1 and it is significantly reduced in the reacting cases with temperature-dependent transport properties. By comparing cases 4, 6 and 7 it can be seen that the heat release parameter is not as important to the change in K_s as the magnitude of the mean reaction rate peak. On the contrary, the dilatational kinetic energy is amplified during the time when the reaction is important (figure 6b). This amplification is strongly influenced by the heat release parameter, as the results obtained for case 4 are significantly larger than those obtained for the other reacting cases. A comparison of cases 2, 5 and 7 indicates that the influence of the reaction is amplified if the mean reaction rate peak occurs at later times. Additionally, the magnitude of the mean reaction rate peak does not appear to influence very much the evolution of K_d (compare cases 6 and 7). The results obtained for case 3 are close to those obtained for case 2 at early times, and become slightly higher at later times.

For non-reacting isotropic turbulence Sarkar *et al.* (1991b) showed that at acoustic equilibrium there is an equipartition between the kinetic and potential components of the compressible energy. This equipartition can be written as $K_d \approx E_p$,

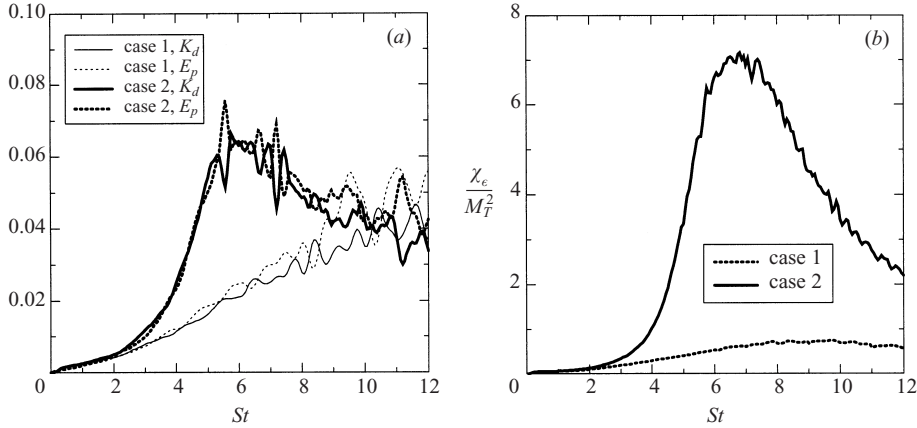


FIGURE 7. (a) Comparison between the kinetic and potential energies of the dilatational components of the velocity. (b) Evolution of the scaled χ_ϵ for the reacting and nonreacting cases.

where $E_p \equiv \langle p'^c \rangle / 2\gamma \langle p \rangle$, and the compressible fluctuating pressure is defined by $p'^c = p - \langle p \rangle - p'^I$. The incompressible fluctuating pressure, p'^I , and the solenoidal velocity satisfy the Poisson equation. The equipartition should occur as long as the other time scales of the problem are much larger than the acoustic time scale. Moreover, the simulations of Sarkar *et al.* (1991a) indicate that this equipartition approximately holds for turbulent homogeneous shear flow. For the reacting cases discussed in this paper the reaction time scale is larger than the acoustic time scale at all times. Therefore, as figure 7(a) suggests, the equipartition between K_d and E_p is not significantly affected by the reaction. However, the heat addition substantially modifies the magnitude of K_d (and E_p). Moreover, although $\langle p'_{rms} \rangle / \langle p \rangle$ scales with M_T^2 as in the non-reacting case, its compressible counterpart does not.

Numerical simulations of compressible non-reacting shear flows (Blaisdell *et al.* 1993; Sarkar *et al.* 1991a) show that $\chi_\epsilon \equiv \epsilon_d / \epsilon_s$ becomes independent of the initial compressibility level, after a development time. Using the equipartition between the kinetic and potential energies of the compressible component and assuming $p'_{rms} \sim M_T^2$ and $\chi_\epsilon \sim K_d / K_s$, Sarkar *et al.* (1991b) derived the relation $\chi_\epsilon = \alpha M_T^2$. This relation is supported by the non-reacting shear flow simulations of Blaisdell *et al.* (1993) and Sarkar *et al.* (1991a) with the value of 0.5 for α . Although the equipartition of energy seems to approximately hold for the reacting case, the next two assumptions in deriving the M_T^2 dependence of χ_ϵ (see above) are not valid in the presence of heat release and the evolution of χ_ϵ does not exhibit a M_T^2 dependence (figure 7b). Similar results are obtained for the model proposed by Zeman (1990), which expresses χ_ϵ as a function of M_T and the kurtosis $\langle u_i'^2 u_i'^2 \rangle / \langle u_i' u_i' \rangle^2$. In the presence of heat release, the model prediction deviates significantly from the DNS results.

In order to examine the energy exchange leading to different behaviour of the dilatational terms in the reacting and non-reacting simulations, the transport equations for the solenoidal and dilatational parts of the kinetic energy are considered. The interactions between the components of the kinetic energy in isotropic flows are studied in detail by Kida & Orszag (1990, 1992) for the non-reacting case, and by Jaber & Madnia (1998) and Jaber *et al.* (2000) for the reacting case. Here, we extend this analysis for the case of turbulent shear flow. The scaled transport equations for

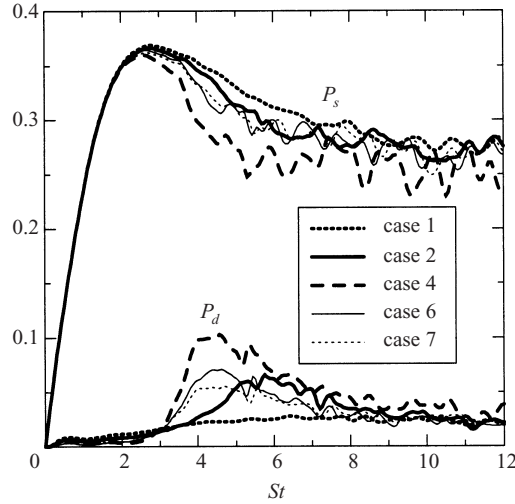


FIGURE 8. Temporal variation of the production terms in the transport equation (3.6) for the dilatational and solenoidal parts of the kinetic energy.

the solenoidal, dilatational, and mean parts of the kinetic energy for this case are

$$\frac{1}{K} \frac{d}{d(St)} K_\alpha = CT_\alpha + AD_\alpha + PD_\alpha + P_\alpha + VD_\alpha + VD1_\alpha. \quad (3.6)$$

The term CT_α arises in equation (3.6) due to the transformation of coordinates. The remaining terms represent the effect of advection, pressure–dilatation, production, viscous dissipation, and viscous dissipation due to the interaction with the mean flow on the volumetric-averaged values of the turbulent kinetic energy components, respectively. The definitions of the terms in equation (3.6) are presented in Appendix B. It should be noted that, consistent with the numerical methodology described in §2.2, AD_α was calculated using the skew-symmetric form of the convective terms. Our results indicate that in both non-reacting and reacting cases the mean component of the kinetic energy and all the terms in its transport equation are negligible compared to their solenoidal and dilatational counterparts. Also $VD_s \approx -\epsilon_s$ and $VD_d \approx -\epsilon_d$ for all cases considered.

Both CT_α and AD_α terms have negligible net effect on the kinetic energy; they only transfer energy between the solenoidal and the dilatational components of K . For the non-reacting case the solenoidal and dilatational parts of both CT_α and AD_α have negative and positive time-averaged values, respectively, indicating a transfer of energy from the solenoidal to the dilatational component of K . However, when the reaction is significant, the two terms change sign and the energy transfer is reversed. Nevertheless, the values of CT_α and AD_α are small compared to the other terms in equation (3.6), so the direct coupling between the solenoidal and dilatational motions is small for the cases considered.

As expected, the solenoidal component of the pressure–dilatation correlation is small compared to its dilatational counterpart for both the non-reacting and reacting cases. Consequently, the energy exchange by reversible work between the kinetic and internal energies occurs primarily through the dilatational motions.

It was shown in §3.1 that the production term is only slightly affected by the heat release. Figure 8 shows, however, that both the solenoidal and the dilatational components of the production term are affected by heat release. While the production

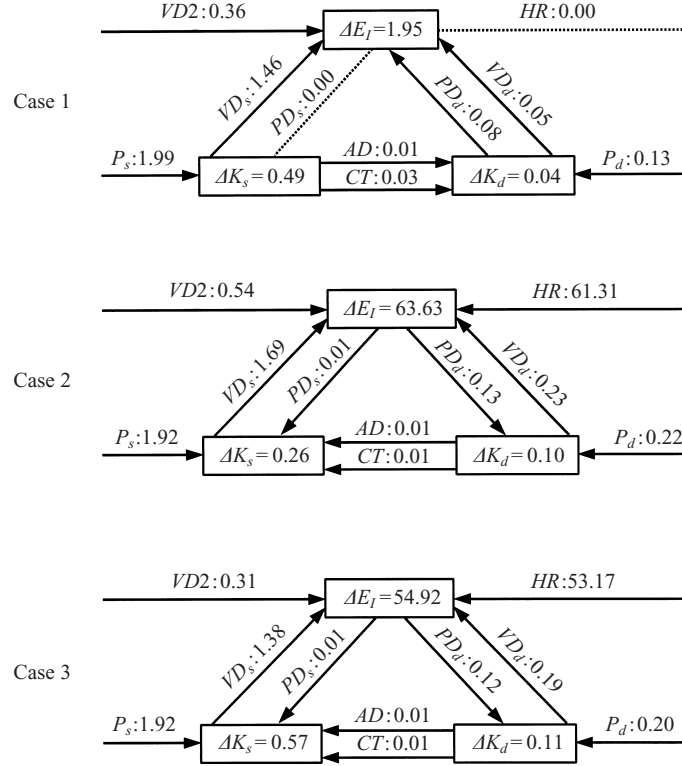


FIGURE 9. Energy flow diagrams for solenoidal and dilatational parts of the turbulent kinetic energy for $2 < St < 8$.

term in the scaled dilatational kinetic energy equation is amplified by the heat release, the production of the solenoidal kinetic energy decreases when the reaction is significant. A comparison among cases with different reaction parameters indicates that the influence of heat release on the solenoidal and dilatational components of the production term primarily depends on the value of Ce .

In order to quantify the contribution of each term in equations (3.2), (3.3) and (3.6) to the energy exchange and the effects of the reaction on this exchange, these equations are integrated from $St = 2$ to $St = 8$. Outside this interval, only 15% of the total area lies under the mean reaction rate for the base case and $\langle w \rangle$ is always smaller than 10% of its maximum value. Thus, most of the reaction occurs during $2 < St < 8$. Figure 9 presents the change in the solenoidal and dilatational parts of the turbulent kinetic energy, internal and modified total energies and the contribution of each term in their scaled transport equations to this change for $2 < St < 8$. Here ΔE_I , ΔE_t , ΔK_s and ΔK_d represent the integrated values of the left-hand side of equations (3.2), (3.3) and (3.6), respectively. The arrows point in the direction of energy transfer. Each arrow represents a term in the transport equations for E_I , E_t and K_x and is labelled with the value of the time integral from $St = 2$ to $St = 8$ for that term.

The results presented in figure 9 are consistent with the previous discussion and show that both components of the kinetic energy are affected by the heat release. However, the modification in the transport properties with the temperature influences mostly the solenoidal part of the kinetic energy. Similar to the evolution of the kinetic energy, its solenoidal part decreases in the reacting case with variable molecular

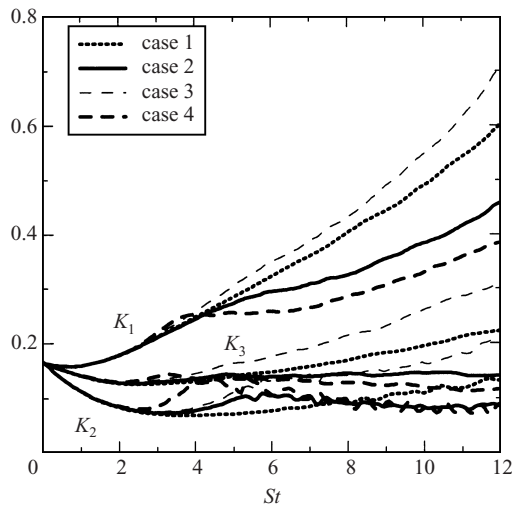


FIGURE 10. Evolution of the turbulent kinetic energy along each coordinate direction.

transport coefficients primarily due to an enhanced viscous dissipation. The average change in the dilatational kinetic energy and all the terms which contribute to this change are not significantly affected by the variation of the transport properties. Compared with the non-reacting case, the dilatational kinetic energy increases due to both an increased production and a transfer of energy from the internal energy by the pressure–dilatation correlation.

3.3. Reynolds stresses

So far we have discussed the heat release effects on the evolution of turbulent kinetic energy and its solenoidal and dilatational components. However, due to the presence of the shear, the initially isotropic flow becomes anisotropic, and it is well known that for the non-reacting case most of the turbulent kinetic energy is in the x_1 -component while the kinetic energy in the direction of the shear is the smallest (Blaisdell *et al.* 1991). In the presence of heat release all three components of the kinetic energy (normal Reynolds stresses) are affected (figure 10). For the reacting cases with variable transport properties the kinetic energy in the x_1 - and x_3 -directions decreases compared to the non-reacting case and it is shown below that this effect can be attributed to an enhanced viscous dissipation in these directions. However, the kinetic energy in the direction of the shear increases during the time when the reaction is important, compared to the non-reacting case. This behaviour, explained below, is related to the enhancement of the energy transfer from the internal energy to the kinetic energy in the x_2 -direction, by the reaction. In the next section, it is shown that in general the explicit dilatational effects in the transport equation for kinetic energy occur primarily in the x_2 -direction.

The kinetic energy in each coordinate direction can be scaled by K to obtain the diagonal components of the Reynolds stress anisotropy tensor, $b_{ij} = \langle \rho u_i'' u_j'' \rangle / \langle \rho u_k'' u_k'' \rangle - \frac{1}{3} \delta_{ij}$. During the time when the reaction is important b_{11} , the highest diagonal component, and b_{22} , the lowest, become closer (Livescu 2001). This indicates that the heat release acts to decrease the anisotropy among the normal stresses. Similar behaviour is obtained for the range of M_0 and S^* examined, although the reaction effects on b_{11} and b_{22} are amplified as the value of S^* increases.

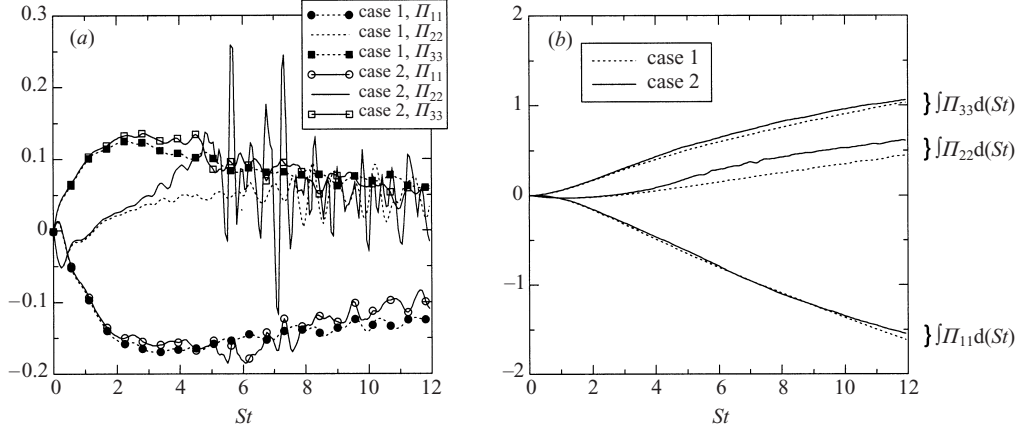


FIGURE 11. Normalized diagonal components of the pressure–strain tensor: (a) time evolution and (b) time integral.

The decrease of the anisotropy among normal stresses due to the reaction was also observed in numerical simulations of reacting mixing layers (Luo 1999).

The scaled transport equations for the kinetic energy components are discussed below:

$$\frac{1}{K} \frac{d}{d(St)} K_1 = P + \Pi_{11} - \epsilon_{11}^d - \epsilon_{11}^s + O(\mu''), \quad (3.7)$$

$$\frac{1}{K} \frac{d}{d(St)} K_2 = \Pi_{22} - \epsilon_{22}^d - \epsilon_{22}^s + O(\mu''), \quad (3.8)$$

$$\frac{1}{K} \frac{d}{d(St)} K_3 = \Pi_{33} - \epsilon_{33}^d - \epsilon_{33}^s + O(\mu''), \quad (3.9)$$

where $K_i = \frac{1}{2} \langle \rho u_i'^2 \rangle$ and the rest of the terms in equations (3.7)–(3.9) are presented in Appendix C. The terms containing μ'' are small for all cases and can be neglected.

Figure 11(a) shows the time variation of the pressure–strain term for the base cases. As expected, the pressure–strain acts to redistribute energy from the x_1 -component of the kinetic energy (the only component with a production term in its transport equation) to the other two components. For both the reacting and the non-reacting cases the pressure–dilatation oscillations shown in the previous sections (figure 3a) are correlated with the evolution of Π_{22} . Although Π_{11} and Π_{33} oscillate in time, the amplitude of the oscillations is much smaller than those of Π_{22} and the results for Π_{11} and Π_{33} obtained for cases 1 and 2 are not very different. The latter observation becomes more clear if the time-integrated values of the pressure–strain terms are considered (figure 11b). Π_{11} and Π_{33} are only slightly affected by the reaction and most of the heat release influence on the pressure–dilatation correlation (which is equal to the sum of three pressure–strain terms) comes from the contribution of Π_{22} .

Both the dilatational and the solenoidal parts of the dissipation tensor are strongly affected by the reaction. Figure 12(a) shows that the magnitude of ϵ_{22}^d is much larger than the magnitude of ϵ_{11}^d and ϵ_{33}^d for both non-reacting and reacting cases, and it is strongly amplified by the heat release. A further increase in the magnitude of ϵ_{22}^d can be obtained by increasing Ce or if the mean reaction rate peaks at later times (Livescu 2001). The largest solenoidal component is ϵ_{11}^s and ϵ_{22}^s is the smallest, as

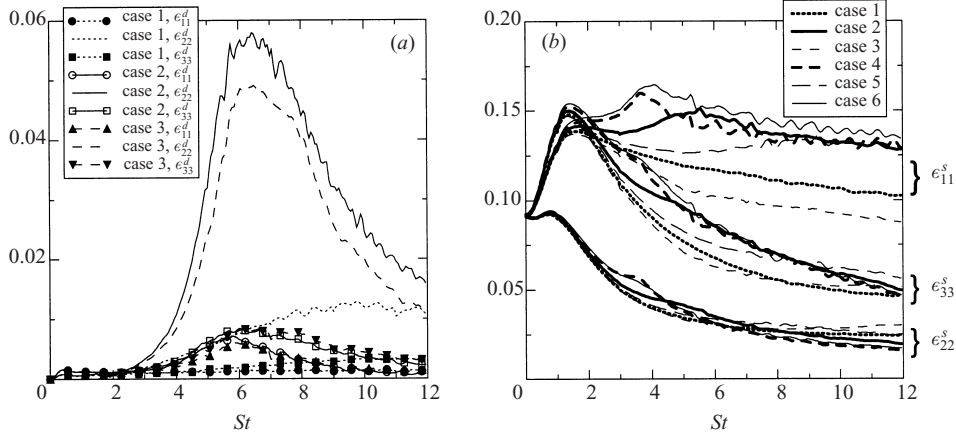


FIGURE 12. Evolution of the normalized diagonal components of (a) dilatational dissipation tensor and (b) solenoidal dissipation tensor.

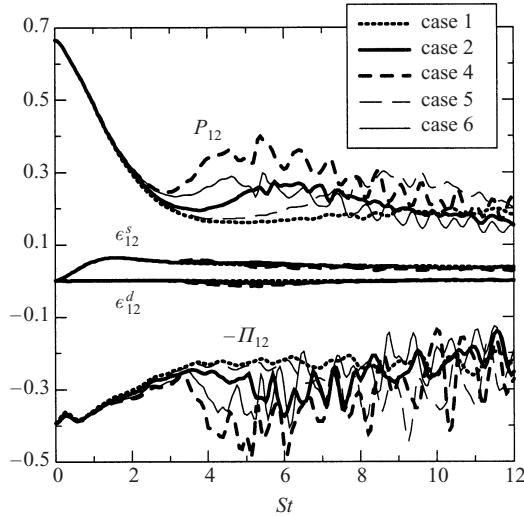


FIGURE 13. Temporal variation of the terms in the transport equation (3.10) for the normalized Reynolds shear stress.

indicated by figure 12(b). Interestingly, the solenoidal dissipation in the x_2 -direction is only slightly affected by heat release, while ϵ_{11}^s is significantly changed.

It was shown in section §3.1 that the production term in the scaled kinetic energy equation is not significantly affected by the heat release, although its solenoidal and dilatational components change in the presence of the reaction. In order to further understand this behaviour, the scaled transport equation for the Reynolds shear stress anisotropy is considered:

$$\frac{d}{d(St)} \frac{-\langle \rho u_1'' u_2'' \rangle}{K} = P_{12} - \Pi_{12} + \epsilon_{12}^d + \epsilon_{12}^s + O(\mu''). \quad (3.10)$$

The terms in equation (3.10) are presented in Appendix C.

Figure 13 presents the time variation of the terms in equation (3.10). Both the solenoidal and the dilatational parts of the viscous term are almost unaffected by

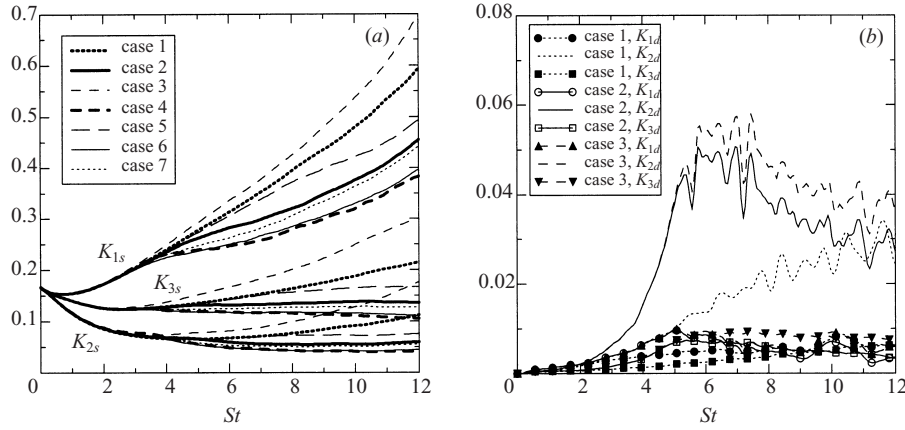


FIGURE 14. Evolution of (a) solenoidal and (b) dilatational components of the turbulent kinetic energy along each coordinate direction.

the heat release. The two important terms in the equation, the production and the pressure–strain terms, increase significantly during the time when the reaction is important. This increase is amplified as Ce increases and it seems little influenced by the magnitude of the mean reaction rate peak or the time when this peak occurs. As figure 13 indicates, the production and pressure–strain terms make an opposite contribution to the right-hand side of equation (3.10) and the net effect to the change in the normalized shear stress is small for all cases considered.

3.4. Solenoidal and dilatational components of the normal stresses

It was shown above that the solenoidal–dilatational decomposition of the kinetic energy is useful in understanding the effects of reaction, since the mechanisms through which the heat of reaction changes these components are different. The kinetic energy in each direction is also affected differently by the reaction. Moreover, if the solenoidal and dilatational parts of the kinetic energy in each direction are considered, then the effects of heat release can be better isolated and understood. It should be noted here that $K_i = K_{id} + K_{is} + \langle W_i W_{(i)d} \rangle$ (no summation over i). Consistent with the non-reacting simulations of Blaisdell *et al.* (1991) the cross Reynolds stresses are small for both reacting and non-reacting cases and are of the same order as K_{1d} and K_{3d} . Additionally, as is shown below, their overall contribution to the energy transfer is negligible.

The solenoidal part of the kinetic energy in each coordinate direction is larger than its dilatational counterpart and, as figure 14(a) shows, is strongly affected by the reaction. In both reacting and non-reacting cases the largest solenoidal component is the solenoidal kinetic energy in the x_1 -direction, K_{1s} , and the smallest is K_{2s} . Similar to the results obtained for K_s , the evolution of the solenoidal components exhibit little sensitivity to the value of the heat release parameter (compare cases 4 and 6) although it appears to depend on the magnitude of the mean reaction rate peak (compare case 7 with cases 4 and 6).

However, the dilatational part of the kinetic energy has a very different behaviour (figure 14b). For both the reacting and non-reacting cases K_{2d} becomes the only important dilatational component of the kinetic energy after the development time. While K_{2d} increases during the simulation for case 1, for the reacting cases it is significantly amplified during the time when the reaction is important. The strong

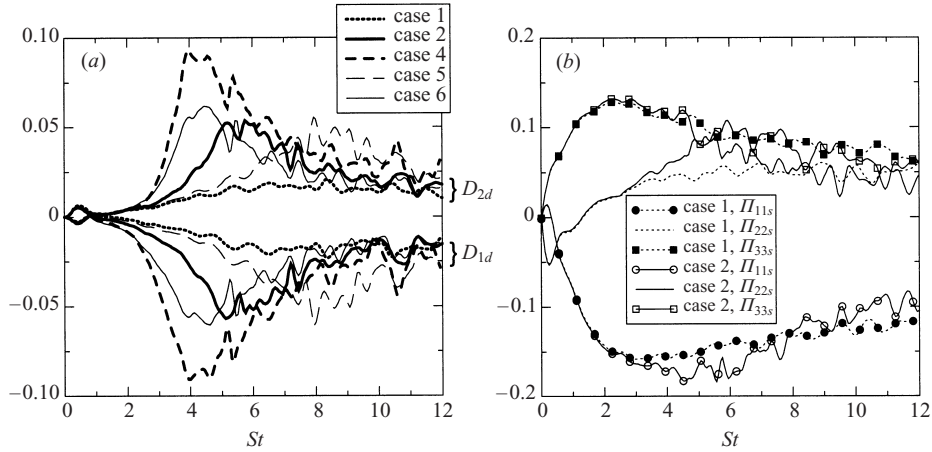


FIGURE 15. Temporal variation of (a) dynamic terms and (b) solenoidal pressure–strain components in equation (3.11).

anisotropy among the dilatational components of the kinetic energy in favour of the x_2 -component was first recognized for non-reacting shear flows by Blaisdell *et al.* (1991). The present results confirm the previous findings and show that the heat release amplifies even more the x_2 -component of the dilatational kinetic energy. This behaviour is related to the spatial structure of the scalar field in the presence of the shear. The scalar field initially composed of non-premixed blobs is distorted by the mean shear and tends to align in parallel layers at a small positive angle with respect to the (x_1, x_3) -plane. The reaction takes place mostly at the interface of the scalar blobs and the heat of reaction produces local expansion zones. The result is an amplification primarily of the x_2 -component of the dilatational energy.

In order to understand how the solenoidal and dilatational components of the kinetic energy in each coordinate direction are coupled and affected by the heat release, their transport equations are considered (no summation over i):

$$\frac{1}{K} \frac{d}{d(St)} K_{i_x} = D_{i_x} + AD_{i_x} + \Pi_{i(i)x} + P_{i_x} + VD_{i_x} + VD1_{i_x} \quad (3.11)$$

The terms in equation (3.11) are presented in Appendix D. It should be noted that the transport equations for the dilatational and solenoidal parts of the kinetic energies in each direction are coupled through dynamical terms, D_{i_x} . These terms represent correlations between the solenoidal (dilatational) velocity and dilatational (solenoidal) acceleration, respectively. By comparing equations (3.11) and (3.6) it can be observed that $\sum_i D_{i_x} = CT_\alpha$. Furthermore, the results indicate that $D_{i_x} \approx -D_{id}$. Figure 15(a) shows the time evolution of D_{1d} and D_{2d} . The x_3 -component is small compared to the other two components for all cases, and, for clarity, is not shown in figure 15(a). Except for very early times, D_{1d} is always negative and D_{2d} always positive, so the energy is transferred from the dilatational to the solenoidal component in the x_1 -direction and in vice versa in the x_2 -direction. During the time when the reaction is significant D_{1d} and D_{2d} increase their magnitude as Ce increases, but the direction of energy transfer is not affected.

The time evolution of the solenoidal components of the pressure–strain tensor is presented in figure 15(b). Since the sum of these components is equal to the solenoidal part of the pressure–dilatation, which is small for the cases considered,

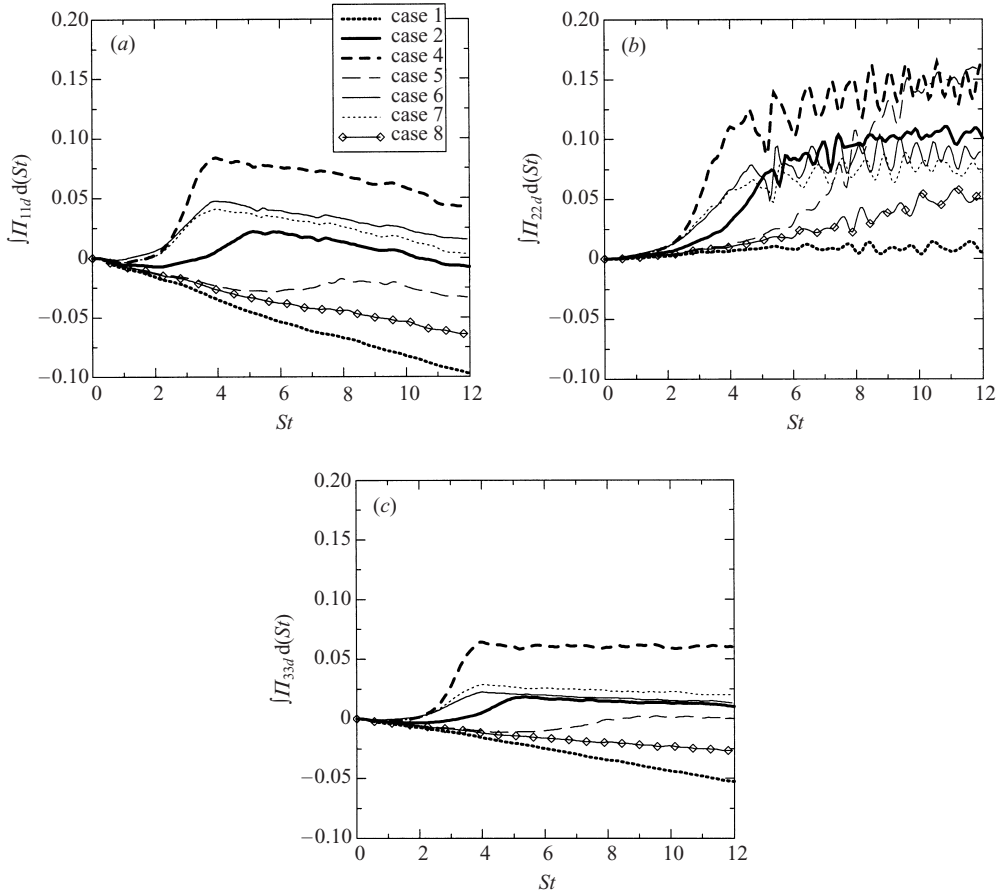


FIGURE 16. Time integral of the dilatational pressure–strain components in (a) the x_1 -direction, (b) x_2 -direction and (c) x_3 -direction.

the role of the solenoidal pressure–strain is only to redistribute the energy among the solenoidal components of the turbulent kinetic energy. For both the reacting and non-reacting cases, the energy is transferred by the solenoidal pressure–strain from the x_1 -component to the x_2 - and x_3 -components of the solenoidal kinetic energy. During the time when reaction is important, the energy transfer in the x_1 - and x_2 -directions by the solenoidal pressure–strain term is amplified. Similar results are obtained for the other cases considered, although the change in the pressure–strain components increases with Ce .

The dilatational components of the pressure–strain tensor are smaller than their solenoidal counterparts, although $\Pi_{22,d}$ has large oscillations with peaks that can approach values close to those of $\Pi_{i(i),s}$. For both the reacting and non-reacting cases, the oscillations in the pressure–dilatation term discussed in the previous sections correspond primarily to oscillations in $\Pi_{22,d}$. This is consistent with the above discussion, indicating that the dilatational effects occur mostly in the direction of the shear. Since the dilatational components of the pressure–strain tensor have positive and negative values, it is useful to examine their time integrals (figure 16). For the non-reacting case, the average contributions in the x_1 - and x_3 -directions to the dilatational motions are always negative and oscillate close to zero for the x_2 -direction. For the reacting

cases with significant heat release, the dilatational components of the pressure–strain tensor increase their values and for the cases considered they transfer energy, on average, from the internal energy to the dilatational kinetic energy. Additionally, figure 16 shows that the time average of $\Pi_{i(i)_d}$ is dependent on the value of Ce . The time when the mean reaction rate peak occurs influences the dilatational pressure–strain components differently. Thus, a comparison between the results obtained for cases 2 and 5 shows that the contribution from Π_{22_d} to the change of the kinetic energy is amplified as the reaction rate peaks at later times (figure 16*b*), while the contributions from the other two components are reduced (figures 16*a* and 16*c*). Thus, the net result for the time average of PD (figure 4) is that the long-time values are slightly dependent on the time when the mean reaction rate peak occurs.

In order to gain a better understanding of the contribution of each term to the energy exchange, equation (3.11) can be integrated during the time when the reaction is significant. The results are presented in figure 17. Both the solenoidal and dilatational kinetic energies in the x_1 -direction increase due to the production terms. However, the energy is transferred from the dilatational to the solenoidal kinetic energies by the velocity–acceleration correlation. On the contrary, the velocity–acceleration correlation transfers energy, on the average, from the solenoidal to the dilatational motions in the x_2 -direction. This transfer is amplified in the presence of heat release, and is not much influenced by the variation in the transport properties (compare cases 2 and 3). This is also the main mechanism of enhancing the x_2 dilatational kinetic energy in both the reacting and non-reacting cases. Moreover, in the presence of heat release the contribution from the pressure–strain term to the variation of the x_2 dilatational motions is significantly enhanced and the dilatational kinetic energy in the x_2 -direction increases compared to the non-reacting case. All the terms contributing to the change of x_1 and x_3 dilatational kinetic energies are influenced by heat release, with small differences between the results obtained for cases 2 and 3. However, these contributions cancel each other and the changes in the dilatational kinetic energy in the x_1 - and x_3 -directions are not significantly affected by the reaction. The results presented remain qualitatively the same for all cases considered and also for the range of M_0 or S^* examined.

4. Summary and conclusions

Direct numerical simulations are conducted of chemically reacting homogeneous compressible shear flows under non-heat-releasing and heat-releasing (exothermic) non-premixed reacting conditions. The chemistry is modelled with a single-step irreversible reaction with Arrhenius-type reaction rate. Simulations are carried out with different values of the parameters which control the reaction rate and the amount of heat released in the flow. The conclusions drawn from the results of these simulations should be considered with the caveat that they are established only in the range of parameters and within the time durations considered in the present simulations.

The energy exchange between internal, E_I , and turbulent kinetic, K , energies is examined and the influence of heat of reaction is assessed. By considering the scaled transport equations for E_I and K , the role of different terms in the energy exchange is identified. It is found that the heat release influences the growth of the turbulent kinetic energy primarily through temperature-induced changes in the solenoidal dissipation and the modifications of the explicit dilatational terms (pressure–dilatation and dilatational dissipation). Additionally, the heat-release-induced changes in the production term play a less important role in the evolution of the turbulent kinetic

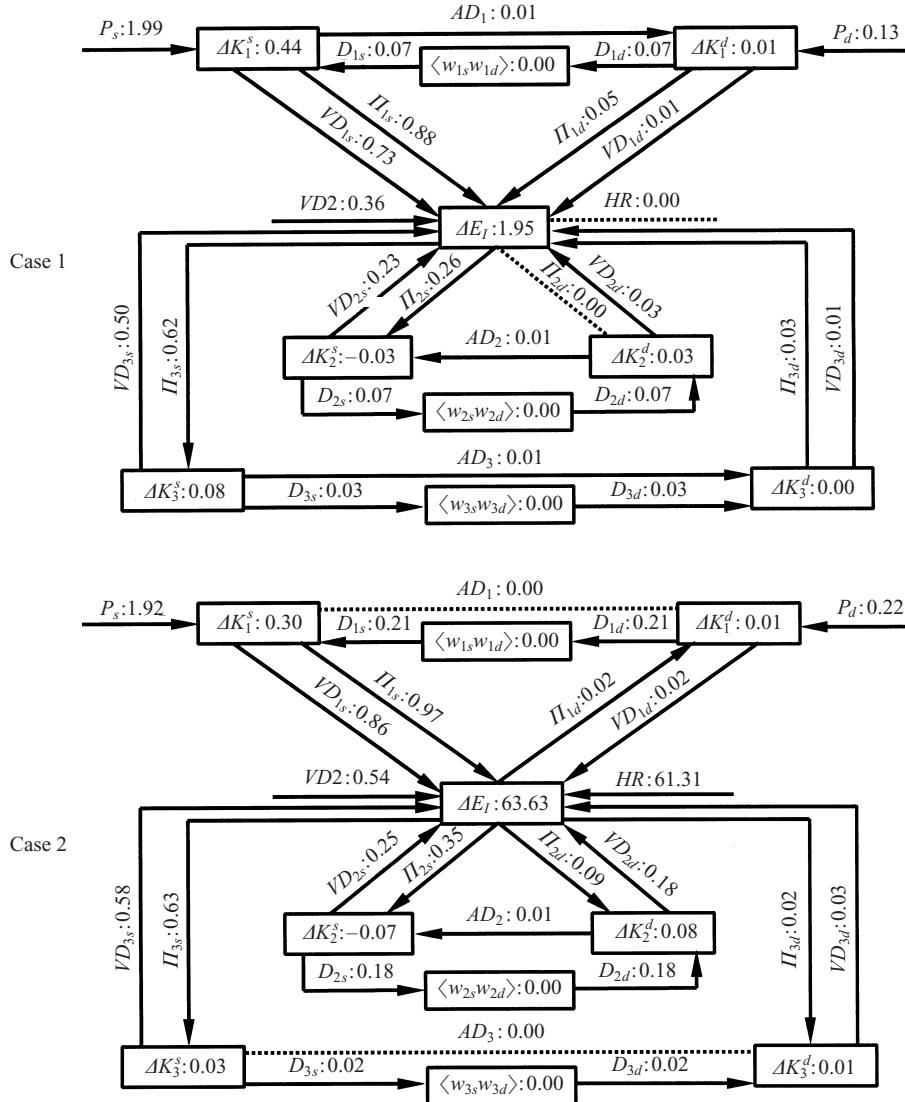


FIGURE 17. For caption see facing page.

energy for all cases considered. To further analyse this behaviour, the scaled transport equation for the production term is considered. The two important terms in this equation, pressure–strain and production, are affected by the heat release. However, since they make opposite contributions to the rate of change of the normalized shear stress, the net effect is small for the cases considered.

Since the heat of reaction directly influences the explicit dilatational terms in the kinetic energy equation, a solenoidal–dilatational decomposition of the kinetic energy (K_s and K_d , respectively) can better reveal the influence of heat release on the flow. It is found that the heat release changes the solenoidal and dilatational velocity fields differently. Thus, during the time when the reaction is important, the production of K_s decreases, while the production of K_d increases. Additionally, since most of the pressure–dilatation contribution goes into the dilatational kinetic energy, K_d increases compared to the non-reacting case. The advection and the coordinate transformation

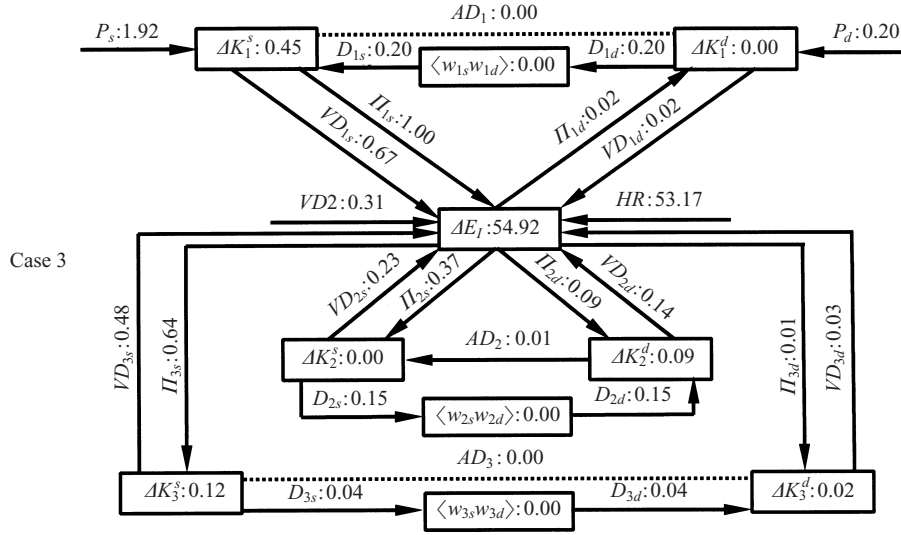


FIGURE 17. Energy flow diagrams for the solenoidal and dilatational turbulent kinetic energy components along each coordinate direction.

terms in the transport equations for K_s and K_d are responsible for the direct coupling between the solenoidal and dilatational components of the kinetic energy. Although these terms are modified by the heat of reaction, their magnitudes remain small compared to other terms. This results in a weak coupling between the solenoidal and dilatational fields for the cases considered.

The examination of the evolution of the turbulent kinetic energy and its solenoidal and dilatational components is useful for the analysis of the flow. However, the velocity field is not isotropic and the heat release affects the kinetic energy differently in each direction. The results show that in all reacting cases, the kinetic energy in the x_2 -direction increases compared to the non-reacting case, during the time when the reaction is important. This is different from the evolution of the kinetic energies in the x_1 - and x_3 -directions, which significantly decrease their magnitudes compared to the non-reacting case. The increase in K_2 is due to an amplification of the dilatational kinetic energy in the x_2 -direction. More generally, it is shown that the explicit dilatational effects occur primarily in the direction of the shear for both non-reacting and reacting cases. For the reacting cases, due to the preferential alignment of the scalar structures with the direction of the shear, this effect is amplified.

Although the dilatational and solenoidal parts of the kinetic energy are only weakly coupled, their components in the x_1 - and x_2 -directions are strongly coupled. This coupling is made through correlations between the solenoidal (dilatational) velocity and dilatational (solenoidal) acceleration, respectively. For all the reacting and the non-reacting cases considered these velocity–acceleration correlations, D_{i_z} , transfer energy from the dilatational to the solenoidal parts of the x_1 -component of the kinetic energy, and in the opposite direction for the x_2 -component. As the value of Ce increases, the magnitudes of D_{i_z} terms are increased but their sign remains the same.

Due to the two-way coupling between the reaction and turbulence, both the magnitude of the mean reaction rate peak and the time when this peak occurs are important for the evolution of the turbulent kinetic energy. The sensitivity of the energy transfer among different types of energy to these parameters as well as

on the amount of heat released in the field is assessed by considering simulations with different values of Ce , Da and k_{0s} . It is found that the change in the explicit dilatational terms is directly influenced by the amount of heat injected into the flow. Additionally, the effects of heat release on these terms are amplified if the reaction occurs at later times. However, the solenoidal dissipation and its components in each direction are not very sensitive to the value of Ce . As a result, the solenoidal turbulent kinetic energy depends weakly on Ce .

Since the explicit dilatational terms in the kinetic energy equation are important for understanding the energy exchange in the turbulent reacting shear flow, the performance of the existing non-reacting models for these terms was assessed for the reacting case. In general, the models examined for the pressure–dilatation and dilatational dissipation do not work well in the presence of heat release. This is partly because neither these terms nor the pressure fluctuations can be described in terms of only one parameter (i.e. M_T). However, some of the assumptions employed for the non-reacting models seem to hold also for the reacting cases considered (e.g. the equipartition between the kinetic and potential components of the dilatational energy) and might be helpful for devising models for turbulent reacting flows.

In this paper the influence of heat release on the energy exchange has been investigated. All the conclusions presented above remain valid for the range of initial Mach number ($0.1 < M_0 < 0.6$) and mean shear rate ($4.8 < S^* < 22$) examined.

We are indebted to Professor G. A. Blaisdell for graciously providing us the initial fields of scb96 case from Blaisdell *et al.* (1991) for validating our code. This work is sponsored by the National Science Foundation under Grant CTS-9623178 and by the donors of the Petroleum Research Fund, administrated by the American Chemical Society under Grant 35064-AC9. Computational resources were provided by the San Diego Supercomputer Center, National Center for Supercomputer Applications at the University of Illinois Urbana-Champaign, and the Center for Computational Research at State University of New York at Buffalo.

Appendix A. Terms in the transport equations for kinetic, internal and total energies

The definitions of the terms in the transport equations (3.1)–(3.3) for the turbulent kinetic, internal and total energies are

$$PD = \frac{\langle p' \Delta \rangle}{SK}, \quad (\text{A } 1)$$

$$P = -\frac{\langle \rho u_1'' u_2'' \rangle}{K}, \quad (\text{A } 2)$$

$$HR = \frac{1}{SK} \frac{Ce}{(\gamma - 1)M_0^2} \langle w_p \rangle, \quad (\text{A } 3)$$

$$\begin{aligned} VD &= -\frac{2}{SK Re_0} \left\langle \mu \left(s_{ij} s_{ij} - \frac{\Delta^2}{3} \right) \right\rangle \\ &= -\underbrace{\frac{\tilde{\mu}}{SK Re_0} \langle \omega_i \omega_i \rangle}_{\epsilon_s} - \underbrace{\frac{4}{3} \frac{\tilde{\mu}}{SK Re_0} \langle \Delta^2 \rangle}_{\epsilon_d} - \underbrace{\frac{2}{SK Re_0} \left\langle \mu'' \left(s_{ij} s_{ij} - \frac{\Delta^2}{3} \right) \right\rangle}_{\text{negligible}}, \quad (\text{A } 4) \end{aligned}$$

$$VD1 = - \underbrace{\frac{2}{K Re_0} \langle \mu'' s_{12} \rangle}_{\text{negligible}}, \quad (\text{A } 5)$$

$$VD2 = \frac{2}{K Re_0} \left\langle \mu \left(s_{12} + \frac{S}{2} \right) \right\rangle = -VD1 + \frac{\langle \mu \rangle}{K Re_0} S, \quad (\text{A } 6)$$

and the vorticity vector is defined by: $\omega_i = \epsilon_{ijk} (\partial u'_k / \partial x'_l) B_{lj}$.

Appendix B. Terms in the transport equations for the kinetic energy components

The definitions of the terms in the transport equation (3.6) for the mean, solenoidal and dilatational kinetic energies are

$$CT_s = \frac{\langle W_{1d} W_{2s} \rangle}{K}, \quad (\text{B } 1)$$

$$CT_d = - \frac{\langle W_{1d} W_{2s} \rangle}{K}, \quad (\text{B } 2)$$

$$CT_o = 0, \quad (\text{B } 3)$$

$$AD_\alpha = - \frac{1}{SK} \left\langle \frac{1}{2} \left[\frac{1}{\sqrt{\rho}} \left(\frac{\partial (W_j W_i)}{\partial x'_k} - W_i \frac{\partial W_j}{\partial x'_k} + W_j \frac{\partial W_i}{\partial x'_k} \right) B_{kj} + W_i \Delta \right] W_{iz} \right\rangle, \quad (\text{B } 4)$$

$$PD_\alpha = - \frac{1}{SK} \left\langle \frac{1}{\sqrt{\rho}} \frac{\partial p'}{\partial x'_k} B_{ki} W_{iz} \right\rangle, \quad (\text{B } 5)$$

$$P_\alpha = - \frac{\langle W_2 W_{1z} \rangle}{K}, \quad (\text{B } 6)$$

$$VD_\alpha = \frac{2}{SK Re_0} \left\langle \frac{1}{\sqrt{\rho}} \frac{\partial}{\partial x'_k} B_{kj} \left[\mu \left(s_{ij} - \frac{1}{3} \Delta \delta_{ij} \right) \right] W_{iz} \right\rangle, \quad (\text{B } 7)$$

$$VD1_\alpha = \frac{1}{K Re_0} \left\langle \frac{1}{\sqrt{\rho}} \left[W_{1z} \frac{\partial \mu}{\partial x'_k} B_{k2} + W_{2z} \frac{\partial \mu}{\partial x'_k} B_{k1} \right] \right\rangle. \quad (\text{B } 8)$$

Appendix C. Terms in the Reynolds stresses transport equations

The definitions of the terms in the transport equations for the normal (equations (3.7)–(3.9)) and shear (equation (3.10)) stresses are

$$P_{12} = \frac{\langle \rho u_2'^2 \rangle}{K} - \left(\frac{\langle \rho u_1' u_2' \rangle}{K} \right)^2, \quad (\text{C } 1)$$

$$\Pi_{11} = \frac{1}{SK} \left\langle p' \frac{\partial u_1'}{\partial x'_k} B_{k1} \right\rangle, \quad (\text{C } 2)$$

$$\Pi_{22} = \frac{1}{SK} \left\langle p' \frac{\partial u_2'}{\partial x'_k} B_{k2} \right\rangle, \quad (\text{C } 3)$$

$$\Pi_{33} = \frac{1}{SK} \left\langle p' \frac{\partial u_3'}{\partial x'_k} B_{k3} \right\rangle, \quad (\text{C } 4)$$

$$\Pi_{12} = \frac{1}{SK} \left\langle \left\langle p' \left(\frac{\partial u_1''}{\partial x_k'} B_{k2} + \frac{\partial u_2''}{\partial x_k'} B_{k1} - \frac{\langle \rho u_1'' u_2'' \rangle}{K} \Delta \right) \right\rangle \right\rangle, \quad (C5)$$

$$\epsilon_{11}^d = \frac{4}{3} \frac{\tilde{\mu}}{SK Re_0} \left\langle \Delta \frac{\partial u_1''}{\partial x_k'} B_{k1} \right\rangle, \quad (C6)$$

$$\epsilon_{22}^d = \frac{4}{3} \frac{\tilde{\mu}}{SK Re_0} \left\langle \Delta \frac{\partial u_2''}{\partial x_k'} B_{k2} \right\rangle, \quad (C7)$$

$$\epsilon_{33}^d = \frac{4}{3} \frac{\tilde{\mu}}{SK Re_0} \left\langle \Delta \frac{\partial u_3''}{\partial x_k'} B_{k3} \right\rangle, \quad (C8)$$

$$\epsilon_{12}^d = \frac{4}{3} \frac{\tilde{\mu}}{SK Re_0} \left\langle \Delta \left[\frac{\partial u_1''}{\partial x_k'} B_{k2} + \frac{\partial u_2''}{\partial x_k'} B_{k1} - \frac{\langle \rho u_1'' u_2'' \rangle}{K} \Delta \right] \right\rangle, \quad (C9)$$

$$\epsilon_{11}^s = \frac{\tilde{\mu}}{SK Re_0} \left\langle -\omega_3 \frac{\partial u_1''}{\partial x_k'} B_{k2} + \omega_2 \frac{\partial u_1''}{\partial x_k'} B_{k3} \right\rangle, \quad (C10)$$

$$\epsilon_{22}^s = \frac{\tilde{\mu}}{SK Re_0} \left\langle -\omega_1 \frac{\partial u_2''}{\partial x_k'} B_{k3} + \omega_3 \frac{\partial u_2''}{\partial x_k'} B_{k1} \right\rangle, \quad (C11)$$

$$\epsilon_{33}^s = \frac{\tilde{\mu}}{SK Re_0} \left\langle -\omega_2 \frac{\partial u_3''}{\partial x_k'} B_{k1} + \omega_1 \frac{\partial u_3''}{\partial x_k'} B_{k2} \right\rangle, \quad (C12)$$

$$\epsilon_{12}^s = \frac{\tilde{\mu}}{SK Re_0} \left\langle \omega_3 \left(\frac{\partial u_1''}{\partial x_k'} B_{k1} - \frac{\partial u_2''}{\partial x_k'} B_{k2} \right) - \omega_1 \frac{\partial u_1''}{\partial x_k'} B_{k3} + \omega_2 \frac{\partial u_2''}{\partial x_k'} B_{k3} - \frac{\langle \rho u_1'' u_2'' \rangle}{K} \omega_i \omega_i \right\rangle. \quad (C13)$$

Appendix D. Terms in the decomposed normal stresses transport equations

The definitions of the terms in the transport equations (3.11) of the decomposed normal stresses are

$$D_{i_s} = -\frac{1}{SK} \left\langle W_{i_s} \frac{\partial W_{(i_d)}}{\partial t} \right\rangle, \quad (D1)$$

$$D_{i_d} = -\frac{1}{SK} \left\langle W_{i_d} \frac{\partial W_{(i_s)}}{\partial t} \right\rangle, \quad (D2)$$

$$AD_{i_z} = -\frac{1}{2SK} \left\langle \left[\frac{1}{\sqrt{\rho}} \left(\frac{\partial (W_j W_i)}{\partial x_k'} B_{kj} - W_i \frac{\partial W_j}{\partial x_k'} B_{kj} + W_j \frac{\partial W_i}{\partial x_k'} B_{kj} \right) + W_i \Delta \right] W_{(i_z)} \right\rangle, \quad (D3)$$

$$\Pi_{i(i)_z} = -\frac{1}{SK} \left\langle \frac{1}{\sqrt{\rho}} \frac{\partial p'}{\partial x_k'} B_{ki} W_{(i)_z} \right\rangle, \quad (D4)$$

$$P_{1_z} = -\frac{\langle W_2 W_{1_z} \rangle}{K}, \quad (D5)$$

$$P_{2_z} = 0, \quad (D6)$$

$$P_{3_z} = 0, \quad (D7)$$

$$VD_{i_z} = \frac{2}{SK Re_0} \left\langle \frac{1}{\sqrt{\rho}} \frac{\partial}{\partial x_k'} \left[\mu \left(s_{ij} - \frac{1}{3} \Delta \delta_{ij} \right) \right] B_{kj} W_{(i)_z} \right\rangle, \quad (D8)$$

$$VD1_{1_x} = \frac{1}{K Re_0} \left\langle \frac{1}{\sqrt{\rho}} \frac{\partial \mu}{\partial x'_k} B_{k2} W_{1_x} \right\rangle, \quad (D 9)$$

$$VD1_{2_x} = \frac{1}{K Re_0} \left\langle \frac{1}{\sqrt{\rho}} \frac{\partial \mu}{\partial x'_k} B_{k1} W_{2_x} \right\rangle, \quad (D 10)$$

$$VD1_{3_x} = 0. \quad (D 11)$$

REFERENCES

- BALAKRISHNAN, G., SARKAR, S. & WILLIAMS, F. A. 1995 Direct numerical simulation of diffusion flames with large heat release in compressible homogeneous turbulence. *AIAA Paper* 95-2375, 1995.
- BLAISDELL, G. A., COLEMAN, G. N. & MANSOUR, N. N. 1996 Rapid distortion theory for compressible homogeneous turbulence under isotropic mean strain. *Phys. Fluids* **8**, 2692-2705.
- BLAISDELL, G. A., MANSOUR, N. N. & REYNOLDS, W. C. 1991 Numerical simulations of compressible homogeneous turbulence. *Rep. TF-50*. Department of Mechanical Engineering, Stanford University, Stanford, CA.
- BLAISDELL, G. A., MANSOUR, N. N. & REYNOLDS, W. C. 1993 Compressibility effects on the growth and structure of homogeneous turbulent shear flows. *J. Fluid Mech.* **256**, 443-485.
- CHEN, J. H., CANTWELL, B. J. & MANSOUR, N. N. 1989 The effect of Mach number on the stability of a plane supersonic wake. *Phys. Fluids A* **2**, 984-1004.
- CHU, B. T. & KOVASZNY, L. S. G. 1958 Non-linear interaction in a viscous heat-conducting compressible gas. *J. Fluid Mech.* **3**, 494-514.
- DIMOTAKIS, P. E. 1991 Turbulent free shear layer mixing and combustion. In *High Speed Flight Propulsion Systems*. Progress in Astronautics and Aeronautics (ed. S. N. B. Murthy & E. T. Vurran), Vol. 137, Chap. 5, pp. 265-340. AIAA.
- DURBIN, P. A. & ZEMAN, O. 1992 Rapid distortion theory for homogeneous compressed turbulence with application to modelling. *J. Fluid Mech.* **242**, 349-370.
- ERLEBACHER, G., HUSSAINI, M. Y., KREISS, H. O. & SARKAR, S. 1990 The analysis and simulation of compressible turbulence. *Theor. Comput. Fluid Dyn.* **2**, 73-95.
- ESWARAN, V. & POPE, S. B. 1988 Direct numerical simulations of the turbulent mixing of a passive scalar. *Phys. Fluids* **31**, 506-520.
- FAVRE, A. 1965 Equations des gaz turbulents compressibles. *J. Mec.* **4**, 361-421.
- FEIERESEN, W. J., SHIRANI, E., FERZIGER, J. H. & REYNOLDS, W. C. 1982 Direct simulation of turbulent shear flows on the Illiac IV computer: applications to compressible and incompressible modeling. In *Turbulent Shear Flows 3* (ed. L. J. S. Bradbury *et al.*), pp. 309-319. Springer.
- GARG, S. & WARHAFT, Z. 1997 On the small scale structure of simple shear flow. *Phys. Fluids* **10**, 662-673.
- GIVI, P. 1989 Model free simulations of turbulent reactive flows. *Prog. Energy Combust. Sci.* **15**, 1-107.
- GIVI, P. 1994 Spectral and random vortex methods in turbulent reacting flows. In *Turbulent Reacting Flows* (ed. P. A. Libby & F. A. Williams), Chap. 8, pp. 475-572. Academic.
- GIVI, P. & MADNIA, C. K. 1992 Spectral methods in combustion. In *Numerical Modeling in Combustion* (ed. T. Chung), pp. 409-452. Hemisphere.
- GOTTLIEB, D. & ORSZAG, S. A. 1977 *Numerical analysis of spectral methods: Theory and Applications*. SIAM, Philadelphia, PA.
- HAMBA, F. 1999 Effects of pressure fluctuations on turbulence growth in compressible shear flow. *Phys. Fluids* **11**, 1623-1635.
- JABERI, F. A., LIVESCU, D. & MADNIA, C. K. 2000 Characteristics of chemically reacting compressible homogeneous turbulence. *Phys. Fluids* **12**, 1189-1209.
- JABERI, F. A. & MADNIA, C. K. 1998 Effects of heat of reaction on homogeneous compressible turbulence. *J. Sci. Comp.* **13**, 201-227.
- KIDA, S. & ORSZAG, S. A. 1990 Energy and spectral dynamics in forced compressible turbulence. *J. Sci. Comput.* **5**, 85-125.

- KIDA, S. & ORSZAG, S. A. 1992 Energy and spectral dynamics in decaying compressible turbulence. *J. Sci. Comput.* **7**, 1–34.
- KOVASZNAVY, L. S. G. 1953 Turbulence in supersonic flow. *J. Aeronaut. Sci.* **20**, 657–682.
- LELE, S. K. 1994 Compressibility effects on turbulence. *Annu. Rev. Fluid Mech.* **26**, 211–254.
- LEONARD, A. D. & HILL, J. C. 1992 Mixing and chemical reaction in sheared and nonsheared homogeneous turbulence. *Fluid Dyn. Res.* **10**, 273–297.
- LIBBY, P. A. & WILLIAMS, F. A. (ED.) 1994 *Turbulent Reacting Flows*. Academic.
- LIVESCU, D. 2001 Mixing and chemical reaction in compressible turbulence. PhD Thesis, SUNY at Buffalo.
- LIVESCU, D., JABERI, F. A. & MADNIA, C. K. 2000 Passive scalar wake behind a line source in grid turbulence. *J. Fluid Mech.* **416**, 117–149.
- LUO, K. H. 1999 Combustion effects on turbulence in a partially premixed supersonic diffusion flame. *Combust. Flame* **119**, 417–435.
- MAHALINGAM, S., CHEN, J. H. & VERVISCH, L. 1995 Finite-rate chemistry and transient effects in direct numerical simulations of turbulent nonpremixed flames. *Combust. Flame* **102**, 285–297.
- MARTIN, M. P. & CANDLER, G. V. 1998 Effects of chemical reaction on decaying isotropic turbulence. *Phys. Fluids* **10**, 1715–1724.
- MILLER, R. S., JABERI, F. A., MADNIA, C. K. & GIVI, P. 1995 The structure and the small-scale intermittency of passive scalars in homogeneous turbulence. *J. Sci. Comput.* **10**, No. 1, 151–180.
- MOIN, P. & MAHESH, K. 1998 Direct numerical simulation: a tool in turbulence research. *Annu. Rev. Fluid Mech.* **30**, 539–578.
- MOYAL, J. E. 1951 The spectra of turbulence in a compressible fluid; eddy turbulence and random noise. *Proc. Camb. Phil. Soc.* **48**, 329–344.
- NOMURA, K. K. & ELGHOBASHI, S. E. 1992 Mixing characteristics of an inhomogeneous scalar in isotropic and homogeneous sheared turbulence. *Phys. Fluids* **4**, 606–625.
- POPE, S. B. 1990 Computations of turbulent combustion: progress and challenges. In *Twenty-Third Symp. (Intl) on Combustion*, pp. 591–612. The Combustion Institute.
- RISTORCELLI, J. R. & BLAISDELL, G. A. 1997 Consistent initial conditions for the DNS of compressible turbulence. *Phys. Fluids* **9**, 4–6.
- ROGALLO, R. S. 1981 Numerical experiments in homogeneous turbulence. *NASA Tech. Mem.* 81315.
- ROGERS, M. M., MOIN, P. & REYNOLDS, W. C. 1987 The structure of the vorticity field in homogeneous turbulent shear flows. *J. Fluid Mech.* **176**, 33–66.
- SANDHAM, N. D. & REYNOLDS, W. C. 1990 Compressible mixing layer: linear theory and direct simulation. *AIAA J.* **28**, 618–624.
- SARKAR, S. 1995 The stabilizing effect of compressibility in turbulent shear flows. *J. Fluid Mech.* **282**, 163–186.
- SARKAR, S., ERLEBACHER, G. & HUSSAINI, M. Y. 1991a Direct simulation of compressible turbulence in a shear flow. *Theor. Comput. Fluid Dyn.* **2**, 291–305.
- SARKAR, S., ERLEBACHER, G., HUSSAINI, M. Y. & KREISS, H. O. 1991b The analysis and modelling of dilatational terms in compressible turbulence. *J. Fluid Mech.* **227**, 473–493.
- SIMONE, A., COLEMAN, G. N. & CAMBON, C. 1997 The effect of compressibility on turbulent shear flow: a rapid-distortion-theory and direct-numerical-simulation study. *J. Fluid Mech.* **330**, 307–338.
- SOUZA, F. A., NGUYEN, V. A. & TAVOULARIS, S. 1995 The structure of highly sheared turbulence. *J. Fluid Mech.* **303**, 155–167.
- TAVOULARIS, S. & CORRSIN, S. 1981 Experiments in nearly homogeneous turbulent shear flow with a uniform mean temperature gradient. Part 1. *J. Fluid Mech.* **104**, 311–347.
- TAVOULARIS, S. & KARNIK, U. 1989 Further experiments on the evolution of turbulent stresses and scales in uniformly sheared turbulence. *J. Fluid Mech.* **204**, 457–478.
- URNS, S. R. 2000 *An Introduction to Combustion: Concepts and Theory*, 2nd Edn. McGraw-Hill.
- VERVISCH, L. & POINSOT, T. 1998 Direct numerical simulation of non-premixed turbulent flames. *Annu. Rev. Fluid Mech.* **30**, 655–691.
- WILLIAMS, F. A. 1995 *Combustion Theory*, 2nd Edn. Academic.
- ZEMAN, O. 1990 Dilatation dissipation: the concept and application in modeling compressible mixing layers. *Phys. Fluids A* **2**, 178–188.